DNA Replication Checkpoint Signaling Depends on a Rad53–Dbf4 N-Terminal Interaction in *Saccharomyces cerevisiae*

Ying-Chou Chen,*,† Jessica Kenworthy,* Carrie Gabrielse,* Christine Hänni,‡ Philip Zegerman,‡ and Michael Weinreich*,1

*Laboratory of Genome Integrity and Tumorigenesis, Van Andel Research Institute, Grand Rapids, Michigan 49503, †Michigan State University, Genetics Program, East Lansing, Michigan 48824, and ‡Department of Zoology, Wellcome Trust/Cancer Research UK Gurdon Institute, The Henry Wellcome Building of Cancer and Developmental Biology, University of Cambridge, Cambridge CB2 1QN, United Kingdom

ABSTRACT Dbf4-dependent kinase (DDK) and cyclin-dependent kinase (CDK) are essential to initiate DNA replication at individual origins. During replication stress, the S-phase checkpoint inhibits the DDK- and CDK-dependent activation of late replication origins. Rad53 kinase is a central effector of the replication checkpoint and both binds to and phosphorylates Dbf4 to prevent late-origin firing. The molecular basis for the Rad53–Dbf4 physical interaction is not clear but occurs through the Dbf4 N terminus. Here we found that both Rad53 FHA1 and FHA2 domains, which specifically recognize phospho-threonine (pT), interacted with Dbf4 through an N-terminal sequence and an adjacent BRCT domain. Purified Rad53 FHA1 domain (but not FHA2) bound to a pT Dbf4 peptide *in vitro*, suggesting a possible phospho-threonine-dependent interaction between FHA1 and Dbf4. The Dbf4–Rad53 interaction is governed by multiple contacts that are separable from the Cdc5- and Msa1-binding sites in the Dbf4 N terminus. Importantly, abrogation of the Rad53–Dbf4 physical interaction blocked Dbf4 phosphorylation and allowed late-origin firing during replication checkpoint activation. This indicated that Rad53 must stably bind to Dbf4 to regulate its activity.

THE fidelity of chromosome replication depends on checkpoint mechanisms to stabilize stalled forks, regulate origin activation, and repair DNA damage (Hartwell and Weinert 1989; Bartek *et al.* 2004; Segurado and Tercero 2009). In response to replication stress, the replication checkpoint maintains replisome stability and prevents late origins from firing, which allows time for DNA repair and the completion of DNA replication prior to chromosome segregation. Incomplete DNA replication or uncoordinated origin firing following DNA damage can result in genomic instability, cancer predisposition, and premature aging (Branzei and Foiani 2010).

In the budding yeast *Saccharomyces cerevisiae*, activation of the checkpoint sensor kinase Mec1 (vertebrate ATR, Ataxia Telangiectasia and Rad3-related) is triggered at stalled forks or sites of DNA damage (Majka *et al.* 2006; Labib and De Piccoli 2011). Subsequent signal amplification through the Mrc1 or Rad9 adaptors leads to activation of the checkpoint kinase Rad53 (the ortholog of the human tumor suppressor Chk2) (Branzei and Foiani 2009). Rad53 is an integral transducer of various cellular responses to replication stress or DNA damage. Rad53 induces a series of transcriptional responses through MBF-regulated genes (Bastos de Oliveira *et al.* 2012; Travesa *et al.* 2012) and also activates the Dun1 kinase, which promotes the expression of ribonucleotide reductase (RNR) subunits and additional DNA repair genes (Huang *et al.* 1998). In parallel, Rad53 down-regulates the RNR inhibitor Sml1 to increase deoxyribonucleotide levels and facilitate DNA synthesis (Zhao *et al.* 2001). In response to replication fork stalling, Rad53 prevents the activation of late replication origins by phosphorylating two proteins required for the initiation of DNA replication: Dbf4 and Sld3 (Lopez-Mosqueda *et al.* 2010; Zegerman and Diffley 2010; Duch *et al.* 2011). Dbf4 is the regulatory subunit of Cdc7 kinase, which is required to initiate DNA replication at individual origins by phosphorylating the replicative MCM

doi: 10.1534/genetics.113.149740
Manuscript received January 23, 2013; accepted for publication March 21, 2013
Supporting information is available online at http://www.genetics.org/lookup/suppl/doi:10.1534/genetics.113.149740/-/DC1.
[1]Corresponding author: Van Andel Research Institute, 333 Bostwick Ave. NE, Grand Rapids, MI 49503. E-mail: michael.weinreich@vai.org

helicase (Tsuji *et al.* 2006; Francis *et al.* 2009; Randell *et al.* 2010; Sheu and Stillman 2010). Sld3 is also required to activate the MCM helicase by promoting Cdc45–MCM association (Fu and Walter 2010; Boos *et al.* 2011).

Cdc7 requires the Dbf4 regulatory subunit for kinase activity. Dbf4 is expressed in late G_1 phase, peaks during S phase, and is present until early to midmitosis, when it is destroyed by ubiquitin-mediated proteolysis (Cheng *et al.* 1999; Weinreich and Stillman 1999; Ferreira *et al.* 2000; Miller *et al.* 2009). The timing of Dbf4 destruction suggests that Dbf4 has postreplicative functions. Indeed, recent work has shown that Dbf4 prevents premature exit from mitosis and also controls the segregation of homologous chromosomes in meiosis I by a direct interaction with Cdc5, the only Polo-like kinase in budding yeast (Matos *et al.* 2008; Miller *et al.* 2009; Chen and Weinreich 2010). Rad53-mediated phosphorylation of Dbf4 postpones late-origin firing during replication stress (Lopez-Mosqueda *et al.* 2010; Zegerman and Diffley 2010; Duch *et al.* 2011) but Cdc7-Dbf4 kinase activity is reduced only twofold by Rad53-dependent Dbf4 phosphorylation (Weinreich and Stillman 1999). It is clear that Dbf4 is an *in vivo* target of Rad53 and interacts with Rad53 (Kihara *et al.* 2000; Duncker *et al.* 2002; Matthews *et al.* 2012), but the molecular details of the Rad53–Dbf4 interaction and how Rad53 phosphorylation of Dbf4 prevents late-origin activation are unclear.

Rad53 is unique in budding yeast in that it contains two fork-head associated (FHA) domains, termed FHA1 and FHA2, which flank a central kinase domain. FHA domains compose a ubiquitous class of protein–protein interaction modules found in >200 different proteins from yeast to mammals (Mahajan *et al.* 2008). Structural studies show that FHA domains fold into a β-sandwich composed of six-stranded and five-stranded β-sheets (Durocher *et al.* 2000). Four of the five most conserved residues in the domain are situated in substrate-binding loops and contribute to highly selective binding to phospho-threonine (Liang and Van Doren 2008). Oriented peptide library screening identified consensus phospho-threonine peptides for the FHA1 and FHA2 domains, and the structural basis of their interaction with the Rad53 FHA domains was also determined (Liao *et al.* 1999; Durocher *et al.* 2000; Byeon *et al.* 2001). The FHA1 domain preferentially binds peptides containing the consensus sequence pT-x-x-D, but the FHA2 domain prefers an isoleucine residue at the +3 position, pT-x-x-I. FHA domains also make extensive contacts with additional regions of pT-containing proteins to stabilize binding (reviewed by Mahajan *et al.* 2008).

Here we have mapped the Dbf4 residues important for a physical interaction with Rad53. We found that a sequence from residues 100–109, which contained a potential FHA1-binding site (T^{105}-x-x-E), and an adjacent BRCA1 carboxyl-terminal (BRCT) domain both interacted with Rad53. Within full-length Rad53, both Rad53 FHA domains were required to bind Dbf4. Biochemical assays showed that the FHA1 domain (but not FHA2) bound to a Dbf4 pT^{105}-X-X-E peptide in a phosphorylation-dependent manner. Finally, abrogation of the Rad53–Dbf4 physical interaction blocked Dbf4 phosphorylation by Rad53 and allowed late-origin firing in the presence of HU. We suggest that the Dbf4 N terminus binds Rad53 using multiple contacts and that Rad53–Dbf4 binding may be phosphorylation dependent. The Rad53 physical interaction with Dbf4 then promotes phosphorylation of Dbf4 at critical downstream sites to inhibit late-origin firing.

Materials and Methods

Construction of yeast strains, plasmids, and baculoviruses

Plasmids and yeast strains used in this study are listed in Supporting Information, Table S1 and Table S2, respectively. PJ69–4a cells (*MAT***a** *trp1-901 leu2-3,112 ura3-52 his3-200 gal4*Δ *gal80*Δ *LYS2*::*GAL1-HIS3 GAL2-ADE2 met*::*GAL7-lacZ*) were used for two-hybrid experiments. All other strains were derivatives of W303-1A. The natMX4 cassette flanked with *DBF4* target sequences was PCR-amplified from p4339 with primers 5′-CTA TCA ACG GCA ATG TTA TTG AAT CAC TTT CTC ATT CAC CCT TGT ACA TGG AGG CCC AGA ATA CC-3′ and 5′-ATG CAA TTG ATA ATA TAT GGA CGA GTA AAT AAG AGT TAA GTC AAT CAG TAT AGC GAC CAG CAT TC-3′ (Goldstein and McCusker 1999), and transformed into M1261 (*dbf4-NΔ109*). clonNAT-resistant transformants (Werner Bioagents) were confirmed with natMX4 marker and then backcrossed to W303. The epitope-tagged *RAD53* strains were made by the method of Longtine *et al.* (1998). Deletions and point mutations within *DBF4* and *RAD53* were generated by site-directed mutagenesis using the QuikChange system (Stratagene). PCR-amplified *Eco*RI-*Pst*I fragments containing the full-length *RAD53*-coding sequence (1–821), FHA1 domain (1–300), FHA2 domain (483–821), and *DBF4*-coding sequence (66–227) were cloned into the same sites of pGAD-C1 (Clontech) to give the Gal4 activation domain fusions. Rad53 residues 2–164 were cloned on a *Bam*HI-*Xho*I into pET24a-GST for expression of the His_6-GST-FHA1 domain. Construction of baculovirus plasmids encoding wild-type Dbf4, Dbf4-NΔ109, HA-Cdc7, and 3Myc-Cdc5 was previously described (Gabrielse *et al.* 2006). An *Nco*I-*Pst*I fragment containing the full-length *RAD53*-coding sequence (1–821) was cloned into the baculovirus transfer vector pAcSG2. High-titer baculoviruses were generated by transfection of Sf9 cells using the BaculoGold kit (BD Biosciences) followed by plaque purification and virus amplification.

Growth conditions, cell-cycle synchronization, and replication intermediate assays

Yeast cells were cultured in YPD or synthetic complete medium (SCM) as described (Gabrielse *et al.* 2006). To detect replication intermediates (Figure 7), cells were synchronized in G_1 phase with 5 μg/ml α-factor for 3 hr and released into 0.2 M HU for the indicated times. The alkaline gel electrophoresis and probes for the replication origins (*ARS305, ARS501 and ARS603,* Autonomously Replicating

Sequence) were previously described (Mantiero *et al.* 2011). DNA content was analyzed by flow cytometry as previously published (Mantiero *et al.* 2011).

Two-hybrid analysis

Various *DBF4* bait constructs containing the Gal4 DNA-binding domain were transformed with Gal4 activation domain prey plasmids in PJ69–4a and selected on SCM plates lacking tryptophan and leucine. These were spotted at 10-fold serial dilutions on the same plates and also on plates also lacking histidine but containing various concentrations of 3-aminotriazole (3AT) and cultured for 2–3 days at 30°. O-nitrophenyl-β-D-galactoside (Sigma) was used to measure β-galactosidase activity.

Immunoprecipitation from Sf9 cells and Western blotting

Sf9 cells were co-infected with HA-Cdc7, 3Myc-Cdc5, Rad53, and Dbf4 mutants as previously described (Chen and Weinreich 2010). Whole-cell extracts and immunoprecipitates (IPs) were probed with polyclonal antibodies against Cdc7 (1:4000) and Dbf4 (1:1000). Rad53 and 3Myc-Cdc5 were detected with yC-19 (Santa Cruz Biotechnology) and 9E10 antibodies, respectively. Antibodies against Gal4 (729-874) were a gift from K. Melcher (Van Andel Institute).

Protein purification and peptide-binding assays

His_6-GST-FHA1 and His_6-GST-FHA2 domains were induced in BL21(DE3) cells for 3 hr at 30° using 0.5 mM isopropyl 1-thio-β-D-galactopyranoside. Protein purification and the AlphaScreen luminescence proximity assay (PerkinElmer Life Sciences) were previously described (Chen and Weinreich 2010). All peptides used in this study are listed in Table S3.

Results

Rad53 interacts with a sequence preceding the Dbf4 BRCT domain

Dbf4 is a downstream substrate of the Rad53 kinase in the DNA replication checkpoint (Masai *et al.* 1999; Weinreich and Stillman 1999; Lopez-Mosqueda *et al.* 2010; Zegerman and Diffley 2010; Duch *et al.* 2011). In the presence of HU, Rad53 phosphorylates multiple sites within Dbf4 to inhibit late-origin firing. Our previous study showed that deletion of Dbf4 residues from 66 to 109 prevented Rad53-mediated Dbf4 phosphorylation in HU (Gabrielse *et al.* 2006), suggesting that these residues, which are N-terminal to a conserved BRCT domain, played a critical role in the Rad53–Dbf4 interaction.

We used a two-hybrid assay to map the Rad53-binding site within Dbf4. Using a series of Dbf4 N-terminal truncations, we found that a deletion through residue 65 retained the Rad53–Dbf4 interaction (Figure 1A). However, a further deletion to residue 109 (just prior to the BRCT domain) resulted in a complete loss of Rad53 binding. Dbf4 N-terminal residues 66–227 were sufficient to interact with Rad53, but, like full-length Dbf4, a deletion to residue 109 abrogated this interaction (Figure 1B). Therefore, the Dbf4 N terminus contains a separate domain (or domains) that interacts with the Rad53 kinase. Also, a sequence preceding the BRCT domain (*i.e.*, within residues 66–109) is required for that interaction.

Both Rad53 FHA domains are required to interact with a Dbf4 N-terminal region spanning residues 100–227

FHA domains are phospho-threonine-specific protein-binding modules, and recognition of the pT residue requires a conserved arginine residue (Durocher *et al.* 2000; Byeon *et al.* 2001). Alanine substitutions of the corresponding arginine residues in the FHA1 and FHA2 domains (R70A and R605A, respectively) abolished the Dbf4 interaction (Figure 1B). Mutation of either Rad53 residue did not decrease Rad53-GAD protein stability (see below), as shown previously for endogenous Rad53 (Pike *et al.* 2003). These results not only indicate that Rad53 binding to the Dbf4 N terminus relies on both FHA domains, but also suggest that the Rad53–Dbf4 interaction involves phosphorylation-dependent FHA contacts.

To identify the FHA-binding sites in Dbf4, we first verified that the FHA1 (Figure 1C) and FHA2 (Figure S1B) domains could bind Dbf4 residues 66–227 independently. We then tested a series of deletion constructs within residues 66–227 for their ability to bind FHA1 and FHA2. Although Dbf4 constructs as short as 100–227 retained FHA binding, deletions beyond residue 100 completely lost FHA1 (and FHA2) binding. This indicates that a Dbf4 sequence following residue 100 is required for the FHA domain interactions. Although critical Dbf4 residues between 66 and 109 were required for the Rad53 interaction (Figure 1A), an ~40-amino-acid peptide from residues 66 to 109 was not sufficient for the interaction with the FHA1 domain (Figure 1C). This same Dbf4 peptide was sufficient to interact with the Cdc5 Polo-box domain (Figure 1C, bottom), and the Cdc5-binding site has been mapped to Dbf4 residues 83–88 (Miller *et al.* 2009; Chen and Weinreich 2010). Finally, the Dbf4–FHA domain interaction also required the Dbf4 BRCT domain comprising residues ~118–224. Any C-terminal deletion that affected the BRCT domain or point mutants in conserved BRCT residues (F166A and W202A) disrupted the Dbf4–FHA domain interaction. To summarize, Dbf4 residues 100–227 compose a minimal region required to bind Rad53 by a two-hybrid assay, and mutation of residues within the BRCT domain or immediately preceding it disrupted that interaction (Figure 1D and below).

Alanine scanning reveals a possible FHA1-binding site in the Dbf4 N terminus

In oriented peptide library screens, the Rad53 FHA1 and FHA2 domains were shown to selectively bind phosphothreonine (Durocher *et al.* 2000; Byeon *et al.* 2001). Therefore, we mutated each threonine to alanine within Dbf4 residues 100–227, *i.e.*, the minimal Rad53 binding region that we defined (Figure 2, A and B; Figure S7). We found that the T105A or T171A substitutions significantly impaired the

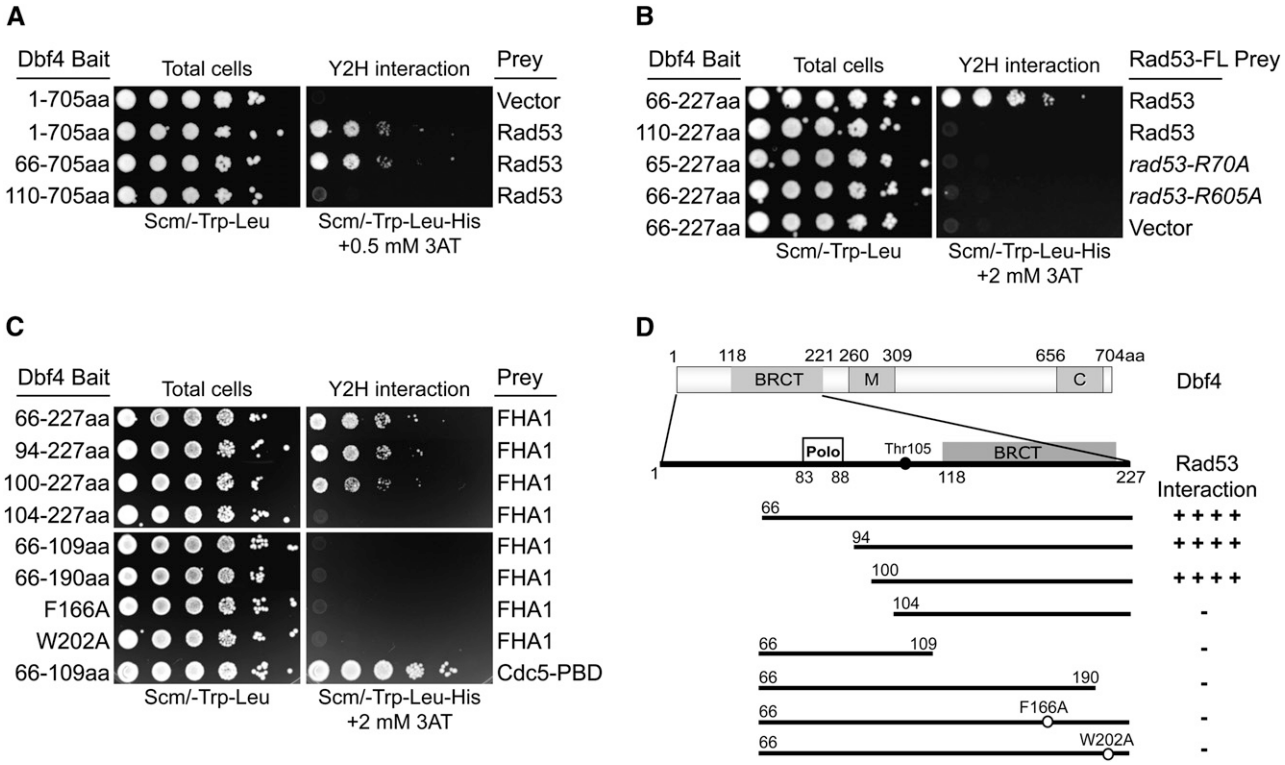

Figure 1 Mapping the interaction between Dbf4 and Rad53. (A) Deletion mutants in otherwise full-length Dbf4 were tested for a two-hybrid interaction with full-length Rad53. Tenfold serial dilutions of saturated cultures were spotted onto SCM-Trp-Leu plates to visualize total cells and SCM-Trp-Leu-His + 2 mM 3AT plates to score the two-hybrid interaction. (B) A Dbf4 N-terminal fragment (residues 66–227) was sufficient for the Rad53 interaction, and this interaction required both the FHA domains. (C) Dbf4 residues 100–227 composed the minimal region for Rad53 FHA1-domain binding. (D) Schematic of the features in Dbf4 are shown, including the Polo-like kinase (Cdc5) binding site, a conserved BRCT domain, and motifs M and C, along with a summary of the Dbf4–FHA1 domain interaction.

Dbf4–FHA domain interactions. The surrounding sequences of these two threonines (**T**^{105}-P-K-**E** and **T**^{171}-I-V-**I**) resemble the binding consensus for the FHA1 (pT-x-x-D) and FHA2 domains (pT-x-x-I), respectively (Durocher *et al.* 2000; Byeon *et al.* 2001). However, a recent crystal structure of the Dbf4 BRCT domain (Matthews *et al.* 2012) showed that the T^{171}-I-V-I sequence forms part of the hydrophobic core of the BRCT domain and is not solvent accessible (T171 is only partially buried). So, although the T^{171}-I-V-I motif conforms to a typical FHA2-binding sequence, this motif is buried and is therefore unlikely to interact with the FHA2 domain directly. However, T105 maps just prior to an α-helix adjacent to the BRCT domain and is solvent accessible.

Using a series of point mutants, we determined the Dbf4 residues between 100 and 114 required for binding the FHA1 and FHA2 domains. In addition to T105, we found that alanine substitutions at V104, E108, L109, or W112 disrupted FHA1 and FHA2 domain binding as summarized in Figure 2C (two-hybrid data in Figure S2). The V104A substitution disrupted the interaction, but V104L had little effect, suggesting a structural role or hydrophobic contact for this residue. The E108A mutation strongly impaired FHA binding and E108K abolished FHA binding. However, a conservative E108D mutation retained FHA binding, suggesting that glutamate and aspartate are interchangeable at this position. As expected for an FHA1-binding consensus site, the Dbf4 residues P106 and K107 at the +1 and +2 positions to T105 were not important for binding, consistent with T^{105}-x-x-E being an FHA1-binding site. Our mutagenesis studies also found that several hydrophobic residues near T105 are important. The loss of interaction caused by the W112A mutation was rescued by substituting F, a bulky hydrophobic residue, suggesting that W112 played a structural role for FHA domain binding. Indeed, W112 falls within an α-helix preceding the BRCT domain and makes hydrophobic contacts with the BRCT domain (Matthews *et al.* 2012). However, L109 may be directly involved in FHA binding, since it is adjacent to E108 and neither the L109A nor L109V mutants interacted with the FHA domains (Figure 2C).

The Rad53 FHA2 domain prefers a pT-x-x-I consensus but can bind to a range of peptides that differ at the +3 position *in vitro* (Liao *et al.* 1999; Wang *et al.* 2000; Byeon *et al.* 2001). The FHA2 domain interaction with Dbf4 required the same residues as the FHA1 domain although the FHA2–Dbf4 interaction was weaker than the FHA1–Dbf4 interaction, as seen previously (Duncker *et al.* 2002). Significant exceptions were that the K107A or K107E substitutions (at the +2 position) substantially enhanced FHA2 binding but did not affect FHA1 binding (Figure 2C). Within full-

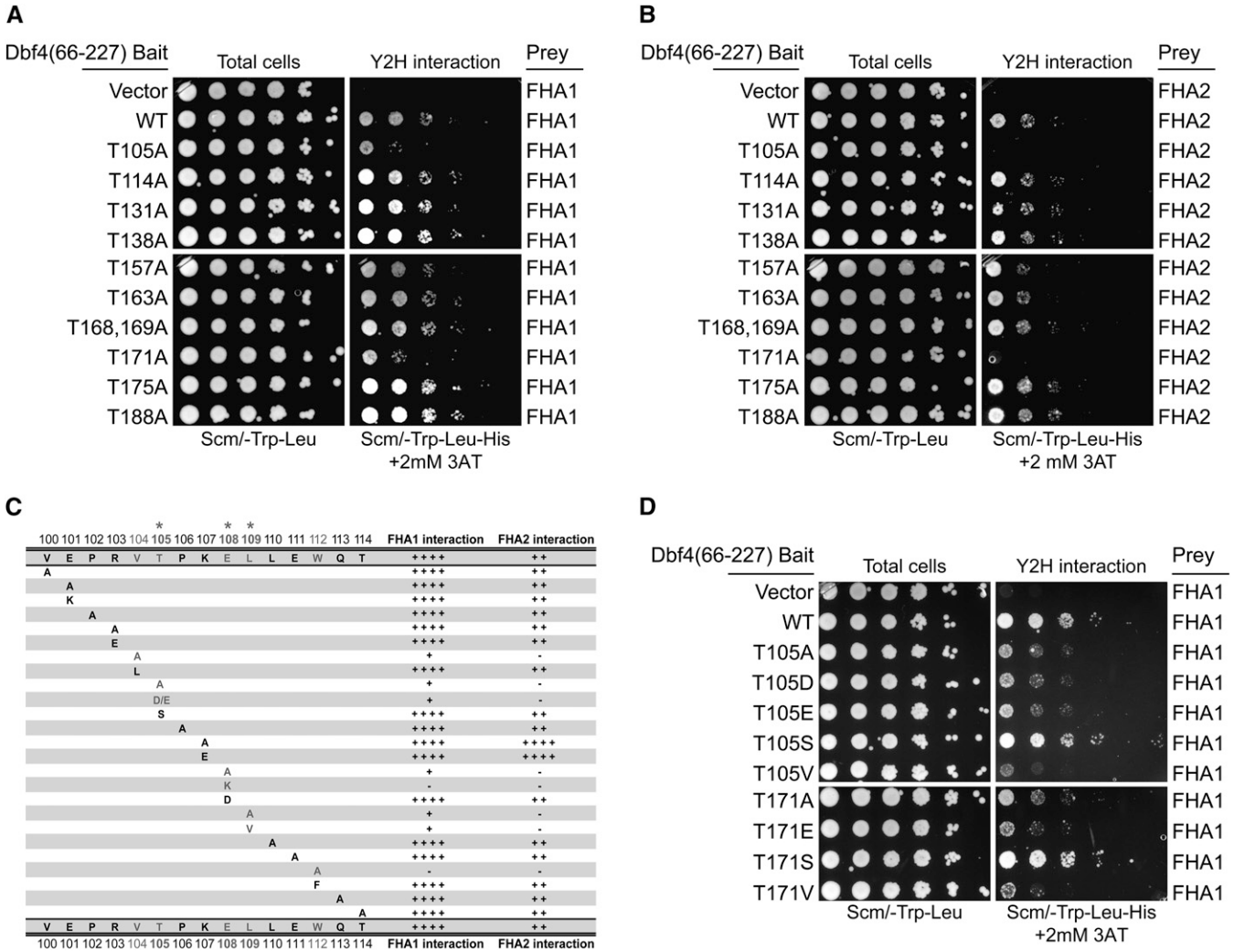

Figure 2 The Rad53 FHA domains required a T^{105}-x-x-E-L motif in the Dbf4 N terminus for interaction. (A and B) An alanine scan of all Dbf4 threonines within the minimal Rad53-binding region (residues 100–227) using two-hybrid assays against FHA1 and FHA2, respectively. (C) Summary of Dbf4 mutants within residues 100–114 for their effect on the interaction of FHA1 and FHA2 domains. Growth assays are shown in Figure S2. (D) Two-hybrid assays showing the effect of additional T105 and T171 mutations on the Dbf4–FHA1 interaction.

length Rad53, the Dbf4-V104A, -T105A, -E108A mutations also impaired binding to Dbf4 but did not eliminate it (Figure S6C).

FHA domains are highly selective for pT so that even acidic substitutions disrupt FHA binding (Durocher *et al.* 1999). In agreement with this, we found that T105D or T105E mutations also disrupted the interaction with FHA1 and FHA2 (Figure 2D). In contrast, both T105S and T171S substitutions had little effect on FHA binding (Figure 2D). If the Rad53 FHA domains selectively bind only pT residues *in vivo*, our mutagenesis data suggest that none of the threonines in the Dbf4 N terminus bind the FHA1/FHA2 domains through a classical pT interaction in yeast.

To further examine the significance of the FHA1–FHA2 interactions, we cloned all 10 remaining FHA domains in the yeast genome and tested their interaction with Dbf4 by the two-hybrid assay. All these proteins were expressed well (not shown); however, none of the 10 domains interacted with Dbf4 (Figure S1C), highlighting the significance of the Rad53 FHA1 and FHA2 interactions. Taken together, our results suggest that both the Rad53 FHA1 and FHA2 domains bind to Dbf4 and that the T^{105}-x-x-E-L sequence is important. However, clearly, other sequences within Rad53 and Dbf4 also contribute to binding.

Dbf4–FHA1 domain interaction is phospho-threonine dependent

To investigate whether the Dbf4–FHA1 domain interaction required phosphorylation of Dbf4 residue T105, we purified the FHA1 domain and tested its ability to bind synthetic Dbf4 peptides using the AlphaScreen proximity assay (Ullman *et al.* 1994). The FHA1 domain bound to the biotinylated Dbf4 peptides containing residues 98–113 but only if T105 was phosphorylated (Figure 3A). In addition, mutation of the conserved R70 to A in FHA1 abolished the interaction with the Dbf4 pT105 peptide. These data indicated

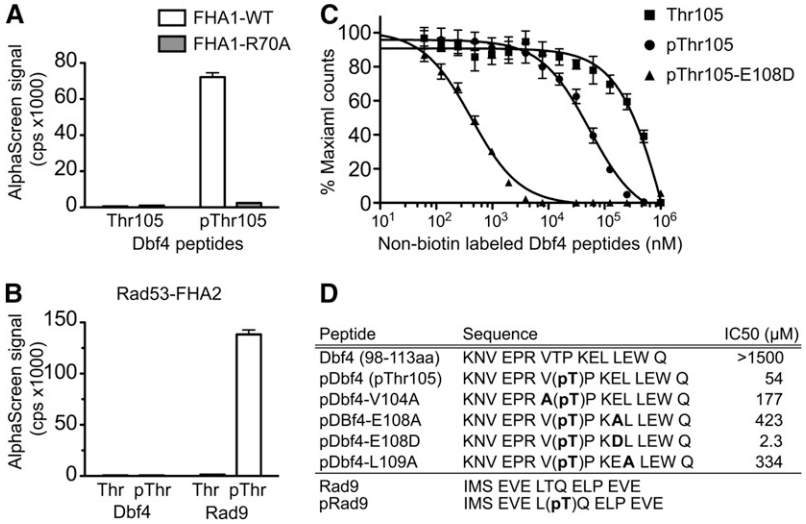

Peptide	Sequence	IC50 (μM)
Dbf4 (98-113aa)	KNV EPR VTP KEL LEW Q	>1500
pDbf4 (pThr105)	KNV EPR V(**pT**)P KEL LEW Q	54
pDbf4-V104A	KNV EPR **A**(**pT**)P KEL LEW Q	177
pDBf4-E108A	KNV EPR V(**pT**)P K**A**L LEW Q	423
pDbf4-E108D	KNV EPR V(**pT**)P K**D**L LEW Q	2.3
pDbf4-L109A	KNV EPR V(**pT**)P KE**A** LEW Q	334
Rad9	IMS EVE LTQ ELP EVE	
pRad9	IMS EVE L(**pT**)Q ELP EVE	

Figure 3 The Rad53 FHA1 domain directly bound to a T105 phosphorylated Dbf4 peptide. (A) Biotinylated Dbf4 peptides (residues 98–113) were tested for interaction with the purified 6His-FHA1 domain using the AlphaScreen Assay. Data represent the average of three independent experiments ± SEM. (B) Purified 6His-FHA2 domain does not interact with the pThr105 Dbf4 peptide, but does selectively bind a Rad9-phosphorylated peptide. (C) The Dbf4–FHA1 domain interaction was competed by nonbiotinylated, T105-phosphorylated Dbf4 peptide (pThr105), a peptide containing the optimal FHA1-binding sequence (pT105-E108D), but not by the T105 (nonphosphorylated) Dbf4 peptide. (D) Summary of peptide sequences and the IC_{50} values determined by competition assays.

that the Dbf4–FHA1 domain interaction required T105 phosphorylation. In contrast, although the FHA2 domain bound efficiently to an optimal Rad9 phosphorylated peptide (Byeon *et al.* 2001), it was unable to bind the same pT105 Dbf4 peptide (Figure 3B). FHA domains bind to pT plus adjacent residues but also make further extensive substrate contacts outside the pT-binding loop (Mahajan *et al.* 2008). Since neither FHA domain bound to Dbf4 residues 66–109 in the two-hybrid assay unless the BRCT domain was included, FHA1 and FHA2 binding to Dbf4 likely required additional FHA–BRCT contacts.

To test whether the additional residues discovered in the two-hybrid screen (V104, E108, and L109) were important for the FHA1–Dbf4 peptide interaction, we used nonbiotinylated peptides to compete FHA1::biotin-pT105 peptide binding. The FHA1::biotin-pT105 interaction was competed by an identical pT105 peptide but not by a nonphosphorylated T105 peptide or by an unrelated serine phosphorylated peptide (Figure 3C and Figure S3A), indicating that the interaction was specific for phospho-T105. The FHA1-pT105 peptide competed with an IC_{50} of 50–60 μM, indicating a moderate FHA1-binding affinity to this peptide. In the yeast two-hybrid assays, we found that E108 and the hydrophobic residues immediately adjacent to the pT^{105}-x-x-E motif were critical for the FHA1 interaction. In agreement with these data, a pT^{105}-x-x A peptide was significantly impaired in its ability to compete the FHA1::biotin-pT105 peptide interaction (Figure S3A). Similarly, alanine substitutions of V104 or L109 within otherwise identical pT105 peptides reduced the ability to compete the FHA1::biotin-pT05 peptide interaction (Figure S3B). Finally, the E108D mutation, which did not affect the Rad53–Dbf4 interaction in the two-hybrid assay and matched the optimal binding sequence for the FHA1 domain, competed the interaction but with a much higher binding affinity (1–5 μM) as shown in Figure 3C. Based on the two-hybrid and biochemical assays, the Rad53 FHA1 domain selectively bound a pT-x-x-E sequence, which closely conforms to an FHA1-binding consensus sequence.

Rad53 and Cdc5 interact with Dbf4-dependent kinase through the Dbf4 N terminus and form a ternary protein complex

Although Dbf4 is well known for its essential role in binding and activating Cdc7 to initiate DNA replication, we recently proposed that Dbf4 also functions as a molecular scaffold to bind and regulate Cdc5 kinase. Dbf4 residues 83–88 directly interact with the Polo-box domain of Cdc5 kinase and are required for Dbf4-dependent kinase (DDK) to bind Cdc5 (Miller *et al.* 2009; Chen and Weinreich 2010). DDK inhibits Cdc5 in the mitotic exit network and also is critical for the spindle position checkpoint (Miller *et al.* 2009; Chen and Weinreich 2010). Once we had defined a distinct binding site for the Rad53 kinase in the Dbf4 N terminus in close proximity to the Cdc5-binding site, we wondered whether Dbf4 could form a ternary complex with the Rad53, Cdc5, and Cdc7 kinases.

To examine the DDK interaction with Cdc5 and Rad53, we employed a baculovirus system to express Rad53, Cdc5, Cdc7, and various Dbf4 derivatives in Sf9 cells. Consistent with previous reports (Miller *et al.* 2009; Chen and Weinreich 2010), Cdc5 was co-immunoprecipitated with wild-type Cdc7-Dbf4 but not with the Cdc7-Dbf4-NΔ109 truncation derivative (Figure 4, middle). Similarly, Rad53 bound to wild-type Cdc7-Dbf4, but not to Cdc7-Dbf4-NΔ109. Both Rad53 and Cdc5 also bound the Cdc7-Dbf4-NΔ65 derivative (Miller *et al.* 2009; Chen and Weinreich 2010; data not shown). These results indicate that the association of Rad53 and Cdc5 with Cdc7-Dbf4 depended on Dbf4 residues from 66 to 109, which contain the Cdc5-binding site (residues 83–88) and a Rad53-binding site (residues 104–109).

The co-immunoprecipitation results suggest two different possibilities. Either DDK exists in two distinct protein complexes (DDK-Rad53 and DDK-Cdc5), or, alternatively, DDK can bind to Cdc5 and Rad53 simultaneously. To clarify this, we asked whether Rad53 bound the DDK–Cdc5 complex by performing a sequential co-immunoprecipitation. We expressed all four proteins in Sf9 cells and immunoprecipitated

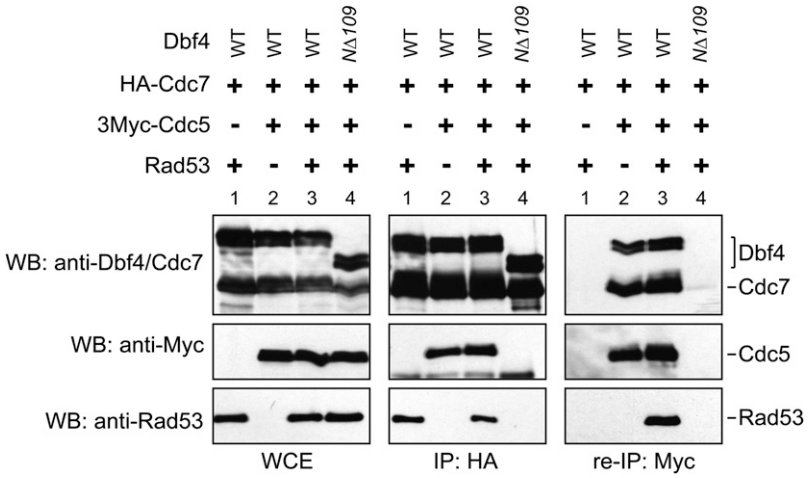

Figure 4 Rad53 and Cdc5 interact with DDK through the Dbf4 N terminus and form a ternary protein complex. HA-Cdc7-Dbf4 complexes were immunoprecipitated from baculovirus-infected Sf9 cells using 12CA5 antibodies and examined for co-immunoprecipitation of Rad53 and 3Myc-Cdc5 by Western blotting (middle). Following 12CA5 immunoprecipitation, proteins were eluted from the beads using HA peptide and subjected to another round of immunoprecipitation by 9E10 antibodies. Rad53 was co-immunoprecipitated with 3Myc-Cdc5 and wild-type DDK but not if Dbf4-NΔ109 was expressed (right).

DDK using the HA tag on the Cdc7 subunit. This procedure immunoprecipitates protein bound to DDK, which includes DDK-(Myc-Cdc5), DDK-Rad53, and presumptive DDK-(Myc-Cdc5)-Rad53 complexes. We then eluted the bound proteins using 1 mM HA peptide and performed a second round of immunoprecipitation using 9E10 monoclonal antibodies to immunoprecipitate only the DDK-(Myc-Cdc5) complexes. Rad53 was present in the second IP (Figure 4, right), indicating that Rad53 forms a ternary complex with Cdc5 and DDK. Together, these results demonstrate that the Dbf4 N terminus acts as a docking site for both Rad53 and Cdc5 and that both kinases can simultaneously associate with DDK.

Rad53 checkpoint defect together with loss of specific Dbf4 N-terminal residues results in synthetic lethality

DDK and *rad53* mutants show a series of complex genetic interactions (Desany *et al.* 1998; Dohrmann *et al.* 1999; Dohrmann and Sclafani 2006; Gabrielse *et al.* 2006). We previously reported that the *dbf4-NΔ109* mutant was synthetically lethal with the *rad53-1* hypomorphic mutant (Gabrielse *et al.* 2006). This is interesting since the *dbf4-NΔ109* mutant exhibits an apparently normal S phase, is not defective for activating early or late replication origins, and is not sensitive to genotoxic agents (Gabrielse *et al.* 2006). Although the Dbf4-NΔ109 protein both binds to and activates Cdc7 normally (Gabrielse *et al.* 2006; Harkins *et al.* 2009), it is defective for binding Cdc5 (Miller *et al.* 2009; Chen and Weinreich 2010) and Rad53 (this study). Therefore, we tested whether the synthetic lethality between *dbf4-NΔ109* and *rad53-1* was due to the loss of the Dbf4–Cdc5 or Dbf4–Rad53 interactions.

We first sequenced the *rad53-1* gene (Weinert *et al.* 1994) and found a single *G653E* point mutation, which is identical to that reported for the *rad53-11* allele (Dohrmann and Sclafani 2006). G653 falls within a loop between the β6 and β7 strands of the FHA2 domain (Figure 5A) and is adjacent to the conserved N655 residue, which plays an important role in substrate recognition (Byeon *et al.* 2001). The *rad53-1* (G653E) or N655A full-length Rad53 mutants were unable to bind the Dbf4 N terminus in the two-hybrid assay like the Rad53-R605A mutant (Figure 1B), but mutation of an adjacent nonconserved residue (T654A) had no effect (Figure 5B). The FHA2 mutants were expressed similarly to wild type with the exception of G653E (Figure 5C), confirming the importance of the FHA2 domain for the Dbf4 interaction. Similar to *rad53-1*, we found that the *rad53-R70A* mutant, which also did not interact with Dbf4 (Figure 1B), was synthetically sick or lethal with *dbf4-NΔ109* but obviously not with *DBF4* (Figure 5D). We also observed synthetic lethality between *dbf4-NΔ109* and the *rad53-K227A* (kinase dead) allele (Figure 5D). Since the *rad53-R70A* and *rad53-G653E* (*rad53-1*) mutants are defective for interacting with DDK to begin with, their synthetic lethality with *dbf4-NΔ109* cannot be due to the further loss of only the Rad53-binding site on Dbf4. The synthetic lethality is likely caused by compromised Rad53 function coupled with loss of a Rad53-independent function of Dbf4 present in the N-terminal 109 residues. We know that this function is not the ability to bind Cdc5, since a *dbf4-Δ82-88* mutant, which is completely defective for binding Cdc5 (Miller *et al.* 2009; Chen and Weinreich 2010), was not synthetically lethal with *rad53-1* or a *rad53Δ* (Figure S4).

Dbf4–Rad53 interaction is separable from a Dbf4 BRCT domain interaction with Msa1

Using the N terminus of Dbf4 as bait (pCG60), we have also identified Msa1 as a Dbf4-interacting protein (Figure 6A). *MSA1* encodes a transcription factor that regulates the timing of G_1-specific gene expression (Ashe *et al.* 2008). *MSA1* was simultaneously reported as a high copy suppressor of temperature-sensitive mutations in *sld2* and *dbp11* (Li *et al.* 2008). Both Sld2 and Dpb11 are required for the initiation of DNA replication and act together with DDK and Sld3 to promote Cdc45 and GINS binding to the MCM helicase, a critical step in MCM helicase activation (Labib 2010).

We found that Dbf4 interacted with Msa1 through its BRCT domain, since both Dbf4 (66–227) and Dbf4 (110–227) proteins interacted with Msa1 similarly, but a W202E (or W202A, not shown) mutation within the BRCT domain blocked binding to Msa1 (Figure 6A). This is in contrast to

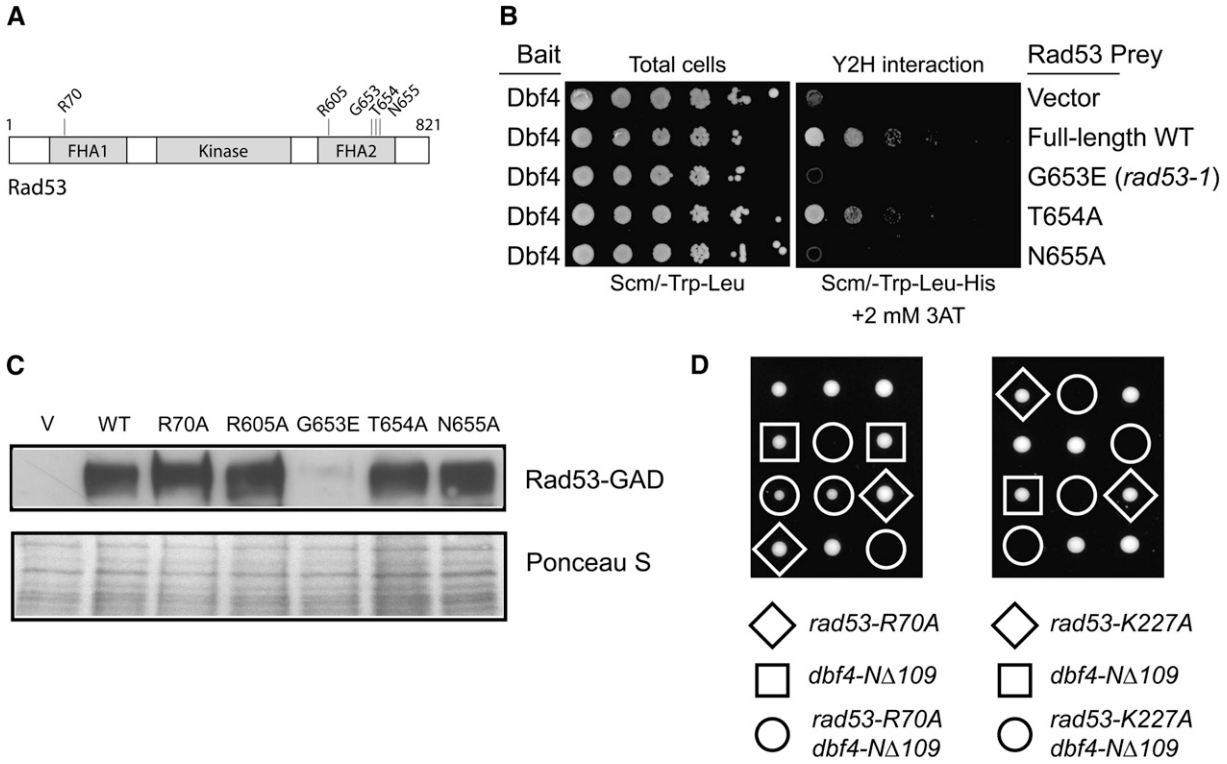

Figure 5 *dbf4-NΔ109* was synthetically lethal with *rad53-R70A*, *rad53-K227A*, and *rad53-G653E*. (A) Schematic diagram of Rad53 showing the mutations studied within the FHA1 and FHA2 domains. (B) The *rad53-G653E* and *rad53-N655A* mutants did not interact with Dbf4 in yeast two-hybrid assays. (C) Western blot of the full-length Rad53-GAD fusion used for two-hybrid analyses and the corresponding FHA domain mutants. The Ponceau S-stained blot is shown below as a loading control. (D) Representative tetrads from diploid strains of genotype *DBF4/dbf4-NΔ109 RAD53/rad53-R70A* and *DBF4/dbf4-NΔ109 RAD53/rad53-K227A* were sporulated and dissected onto YPD plates. Recombinant genotypes are indicated.

Rad53, which does not interact with the BRCT domain alone [*i.e.*, Dbf4 (110–227) in Figure 1, B and C]. We used the Msa1–Dbf4 BRCT interaction as a control to identify specific BRCT residues that contact Rad53. α-Helix 3 (α3) of the Dbf4 BRCT domain is spatially close to α0, which contains the E108, L109, and W212 residues important for binding Rad53 (Figure 2), and directly precedes the BRCT domain (Matthews *et al.* 2012). Therefore, we mutated three positively charged residues within α3 to glutamate and tested the interaction with both Msa1 and Rad53. A K206E mutation disrupted both the Msa1 and Rad53 interactions, and a K212E mutation disrupted neither interaction (Figure 6B). However, the R209E mutation selectively blocked the Dbf4 interaction with Rad53 and thus defined a unique BRCT residue that was important for interaction with Rad53 but not with Msa1 (Figure 6B). Similarly, the Dbf4-E108K and Dbf4-Δ100-109 mutations disrupted the Rad53 interaction (Figure S6C) but have no effect on the Msa1 interaction. Thus, although both Msa1 and Rad53 bind the Dbf4 N terminus, Dbf4 residues from 100 to 109 and R209 are uniquely required for interaction with Rad53.

Dbf4–Rad53 physical interaction is required to inhibit late-origin firing during replication checkpoint activation

In response to replication fork arrest, Rad53 phosphorylates Dbf4 and Sld3 to inhibit late-origin firing, but phosphorylation of either protein is sufficient for this inhibition (Lopez-Mosqueda *et al.* 2010; Zegerman and Diffley 2010). Both studies mapped Rad53 phosphorylation sites on Dbf4 *in vitro*. A *dbf4-4A* mutant that changes 4 serine and threonine Rad53 phosphorylation sites to alanine is sufficient to allow late-origin activation when combined with an *sld3-38A* mutant containing alanine mutations in 38 Rad53 phosphorylation sites (Zegerman and Diffley 2010). We hypothesized that Rad53 regulation of Dbf4 in the replication checkpoint depended on its physical interaction with the Dbf4 N terminus. To test this, we examined whether the combination of a *dbf4-NΔ109* mutant (defective for Rad53 binding, Figure 4) and the *sld3-38A* mutant, which cannot be phosphorylated by Rad53, would allow late-origin firing in the presence of HU. Yeast cells were synchronized in G_1 phase using mating pheromone and then released into S phase in the presence of 0.2 M HU to stall replication forks from early origins. At different time points following release from the G1 arrest, replication intermediates (RI) near ARSs were separated on alkaline gels and detected by Southern blotting with ARS-specific probes to measure replication origin activity. As a control, Rad53 was activated (evidenced by the phosphorylation-dependent mobility shift) in both wild-type and mutant cells following HU treatment (Figure 7A), indicating that neither the *dbf4* nor the *sld3* mutations affect Rad53 checkpoint activation.

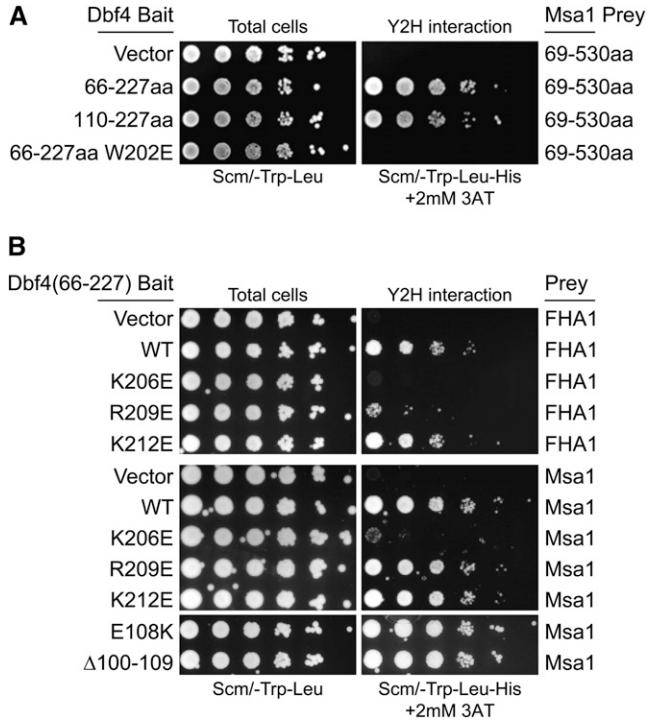

Figure 6 Both Msa1 and Rad53 interacted with the Dbf4 BRCT domain, but the Rad53 interaction was specifically disrupted by an R209E mutation. (A) Two-hybrid assays with indicated Dbf4 bait and Msa1 prey vectors, spotted as in Figure 1. Msa1 interacts with the BRCT domain alone (Dbf4-110-227). (B) Charge reversal mutations of lysine and arginine residues in the BRCT α3 helix (Matthews *et al.* 2012) identify R209E as specifically affecting the Rad53 interaction. Dbf4 residues 100–109 are also uniquely required for the Rad53 interaction (Fig. S6C) but not for the Msa1 interaction.

The early origin, *ARS305*, was active in the wild type, *dbf4-NΔ109*, *dbf4-4A sld3-38A*, and *dbf4-NΔ109 sld3-38A* mutant strains, indicating that induction of the replication checkpoint does not interfere with early origin firing in these cells (Figure 7B). Although Rad53 activation inhibited the firing of late origins *ARS501* and *ARS603* in the wild-type and the single mutants as expected (Lopez-Mosqueda *et al.* 2010; Zegerman and Diffley 2010; Duch *et al.* 2011), replication intermediates were detected at late origins in both the *sld3-38A dbf4-4A* and *sld3-38A dbf4-NΔ109* double mutants to a similar extent (Figure 7, C and D). Thus, the *dbf4-NΔ109* mutant defective for Dbf4-Rad53 binding was similarly defective in preventing late-origin firing in HU as the *dbf4-4A* phosphorylation site allele.

We also tested the effect of Dbf4 N-terminal truncations on the Rad53-dependent phosphorylation of Dbf4 in yeast (seen as a mobility shift in SDS-PAGE gels) after exposure to HU (Weinreich and Stillman 1999; Gabrielse *et al.* 2006; Lopez-Mosqueda *et al.* 2010; Zegerman and Diffley 2010). Log-phase yeast cells ($t = 0$) were treated with HU for 1 and 2 hr to arrest replication forks and induce the replication checkpoint. DDK was immunoprecipitated at each time point and probed for Cdc7 and Dbf4 proteins by Western blotting. Both the wild-type Dbf4 and Dbf4-NΔ94 proteins that retained binding to Rad53 were shifted upon exposure to HU; however, the Dbf4-NΔ109 protein that did not bind Rad53 was not shifted (Figure 7F). These data indicate that loss of Rad53 binding to Dbf4 mediated by critical Dbf4 residues between 95 and 109 caused a significant defect in Dbf4 phosphorylation upon replication fork arrest. Together, these data show that Rad53 must stably interact with Dbf4 through its N-terminal binding site to phosphorylate Dbf4 and inhibit late-origin firing in response to HU.

Discussion

Rad53 FHA domains interact with the Dbf4 N terminus

Multiple groups have reported genetic and physical interactions between *S. cerevisiae* Dbf4 and Rad53 (Dohrmann *et al.* 1999; Weinreich and Stillman 1999; Kihara *et al.* 2000; Duncker *et al.* 2002; Gabrielse *et al.* 2006; Matthews *et al.* 2012) and *Schizosaccharomyces pombe* Dfp1 and Cds1 (Takeda *et al.* 2001; Fung *et al.* 2002). Furthermore, in response to DNA damage human and *Xenopus* DDK are downstream targets of ATR signaling (Costanzo *et al.* 2003; Lee *et al.* 2012). The Dbf4 regulation by checkpoint kinases is broadly conserved since it likely promotes genome stability. Here we have mapped a Rad53-binding site in the Dbf4 N terminus and have shown that a Rad53–Dbf4 physical interaction is critical for regulating late replication origin firing. A minimal Rad53-binding region corresponds to Dbf4 residues 100–227, which compose the Dbf4 BRCT domain (~118–224) and residues immediately N-terminal to this domain. Mutations in either conserved BRCT residues or residues within 100–109 caused defects in Rad53 binding in the two-hybrid assay. Therefore, both the BRCT domain and the region preceding it contributed to Rad53 binding. Despite their different consensus peptide-binding sites, both Rad53 FHA domains interacted with this 100–109 region independently and apparently using the same Dbf4 residues (see below). Mutations that impair phospho-threonine binding in either Rad53 FHA domain blocked interaction with Dbf4, supporting the contention that the Rad53–Dbf4 interaction is mediated by phosphorylation and is multivalent.

Very recently, a crystal structure, the Dbf4 BRCT domain (that included residues 98–221), was described (Matthews *et al.* 2012). These authors also showed that Rad53 interacted with the Dbf4 BRCT domain plus the preceding α-helix using two-hybrid assays; however, none of threonines contained within the structure was shown to directly interact with Rad53. Our study found that residues V104, T105, E108, L109, W112, and R209 were important for the Dbf4–Rad53 interaction and that FHA1 specifically interacted with a T105 phosphorylated Dbf4 peptide *in vitro*. The structure of the Dbf4 N terminus allows us to rationalize this data (Figure 8). T105 is solvent-exposed and occurs within a sequence (T-x-x-E) that closely matches a FHA1-binding site. The E108 residue has the same spatial orientation as T105, and L109 is directly adjacent to E108. The W112 residue

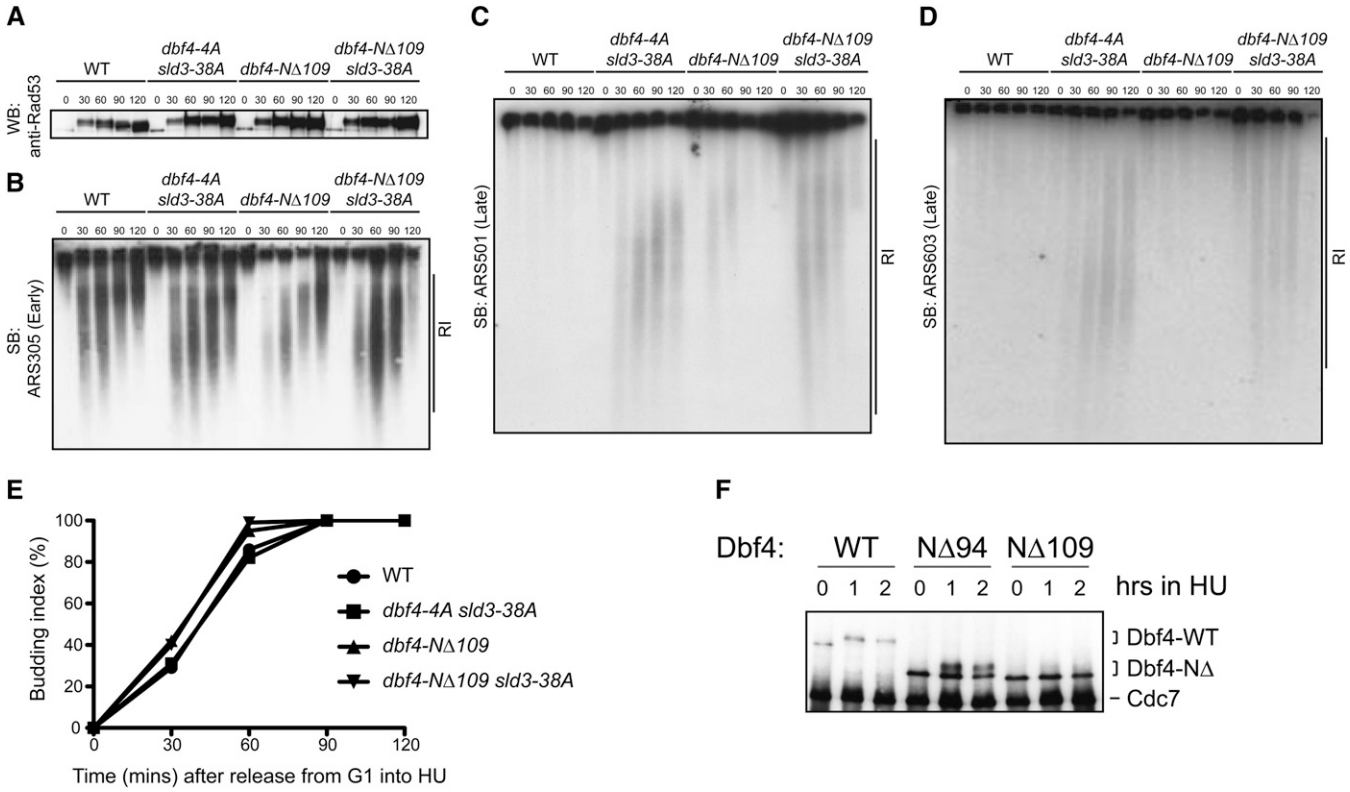

Figure 7 The *dbf4-NΔ109 sld3-38A* double mutant allowed late-origin firing in the presence of HU. (A) Wild-type and mutant cells were synchronized in G_1 phase and released into medium containing 0.2 mM HU for the indicated times. Total protein extracts were examined by Western blotting for Rad53 to assess Rad53 activation (upper band). (B–D) RIs were separated by alkaline gel electrophoresis and detected by Southern blotting to measure the activity of early (*ARS305*) and late (*ARS501* and *ARS603*) origins. Flow cytometry assays indicated all strains arrested in early S phase with HU (not shown); the budding indices are shown in E. (F) Wild-type Cdc7-Dbf4 or N-terminal Dbf4 truncation mutants were immunoprecipitated from asynchronous yeast extracts (t = 0) and after 1 or 2 hr exposure to 0.1 M HU, separated on an SDS gel, and then blotted for Cdc7 and Dbf4 proteins.

packs against L214 present at the C terminus of the BRCT α3 helix. This hydrophobic interaction presumably helps stabilize the α0–α3 orientation and would explain why a W112A mutation disrupts the Dbf4–Rad53 interaction but W112F does not. Finally, R209 on the α3 helix is solvent-exposed and is suitably oriented to interact with an FHA domain bound to α0 or, alternatively, to mediate BRCT–BRCT domain interactions. In a tandem BRCT-BRCT dimer, the α2 helix from one monomer packs against the α1 and α3 helices from the second monomer (Glover *et al.* 2004). Mutation of R209 (but not K212, which is oriented orthogonally to R209 and away from α0) abolished the Dbf4–FHA1 two-hybrid interaction (Figure 6). Since the purified Rad53 FHA1 domain bound only to T105 phosphorylated Dbf4 peptides, these data raise the possibility that the Dbf4 pT^{105}-x-x-E-L motif binds to Rad53 but the Rad53 interaction is further stabilized by additional BRCT domain contacts. T105 phosphorylation is not essential for the Rad53–Dbf4 physical interaction since a Dbf4 quadruple mutant protein (S84A S92A T95A T105A) still underwent a Rad53-dependent shift in HU (Gabrielse *et al.* 2006). Also, a T105A mutation diminished the Dbf4 two-hybrid interaction with full-length Rad53 but did not eliminate it (Figure S6C).

Although the Rad53 FHA2 domain bound to the same sequence as FHA1 in the two-hybrid assay (Figure 2), it did not bind to the 16mer pT-x-x-E peptide *in vitro*, and this sequence does not match the optimal FHA2-binding site consensus. The FHA2 domain might bind to Dbf4 indirectly in the two-hybrid assay, but the FHA2 interaction still occurs in a strain deleted for Rad53 (data not shown), and so it is not mediated by endogenous Rad53. Importantly, none of the other 10 FHA domains encoded in the yeast genome can bind to this Dbf4 sequence (Figure S1C), suggesting again that the FHA2 interaction is biologically relevant. Since a previous study also demonstrated an interaction between FHA2 and Dbf4 using two-hybrid and GST-pull-down assays in yeast (Duncker *et al.* 2002), we suggest that the FHA2 domain interaction with Dbf4 is stabilized *in vivo* by additional contacts within the BRCT domain.

Models for Rad53 binding to Dbf4

We propose several models to explain how Rad53 interacts with Dbf4. Rad53 could use each FHA domain to bind two separate sites within Dbf4, or both Rad53 FHA domains could bind to the same T-x-x-E-L sequence but on different Dbf4 subunits within a Dbf4 dimer. Alternatively, the T-x-x-E-L sequence might help mediate dimerization or other

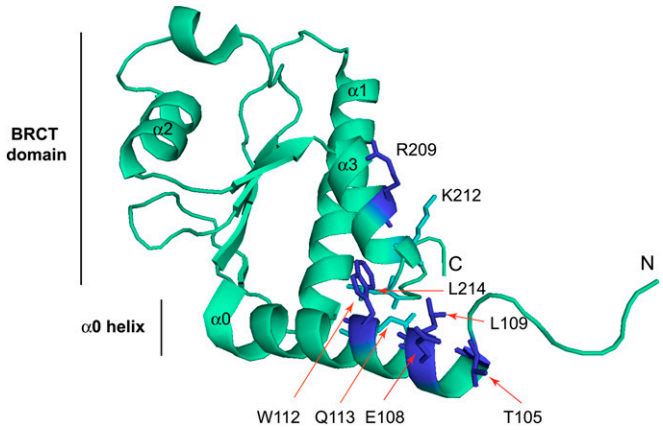

Figure 8 Structural representation of the budding yeast BRCT domain and a preceding α-helix (α0) (both in cyan) using PDB coordinates 3QBZ (Matthews *et al.* 2012). The helices within the BRCT domain are numbered α1, α2, and α3. Five residues that are important for interaction with Rad53 (T105, E108, L109, W112, R209) are colored blue. L214 and Q113, which form a hydrophobic surface with W112, are colored in cyan. K212 is also colored in cyan but is not important for the Rad53 interaction.

structural changes in the BRCT domain necessary to promote Rad53 binding.

Although both Rad53 FHA domains required the same T-x-x-E-L sequence for binding, the BRCT domain is also critical for binding Rad53. It is possible that the Rad53 FHA1 domain binds to pT^{105}-x-x-E –L and that the FHA2 domain binds to another phosphorylated residue in the BRCT domain. This seems unlikely, however, since mutation of every other threonine (Figure 2) or tyrosine residue (Figure S1) (Liao *et al.* 1999; Wang *et al.* 2000; Byeon *et al.* 2001) in the BRCT domain had no effect on FHA1 or FHA2 binding, with the exception of T171 discussed above. Since both the T105S and T171S Dbf4 mutants bound the FHA domains normally, these residues may not interact with Rad53 through "canonical" FHA-pT interactions *in vivo*.

A second model is that the Dbf4 N termini form a dimer using the BRCT domains, and then this Dbf4 dimer provides two T^{105}-x-x-E^{108} sites for the binding of the FHA1 and FHA2 domains separately. DDK or Dbf4 oligomerization has been suggested previously (Shellman *et al.* 1998; Matthews *et al.* 2012). Furthermore, tandem BRCT domains form dimers that bind phospho-S/T motifs (Caldecott 2003; Rodriguez and Songyang 2008), and intermolecular dimerization between BRCT domains has also been described for the DNA repair proteins XRCC1 and Ligase III (Cuneo *et al.* 2011). In support of this model, we saw a significant but weak interaction between Dbf4 N termini using the yeast two-hybrid assay (Figure S5). Substitutions of conserved residues in the Dbf4 BRCT domain as well as deletion of residues 100–109 disrupted the Dbf4–Dbf4 two-hybrid interaction (Figure S5), supporting the idea of BRCT domain dimerization. Arguing against this model is the lack of biochemical data supporting an interaction between the Rad53 FHA2 domain and the pT^{105}-x-x-E peptide; however, as stated above, FHA2 is likely to make additional contacts with the BRCT domain.

Finally, the involvement of residues 100–109 and the T-x-x-E-L motif in particular for Rad53 binding could reflect a requirement for these residues to mediate BRCT structural changes needed for Rad53 binding. Clearly, further biochemical or structural data of FHA1-Dbf4 or Rad53-Dbf4 complexes will be needed to determine exactly how Rad53 interacts with Dbf4.

Dbf4-Rad53 binding is critical for regulation of late-origin activation

Upon sensing DNA damage or replication fork stalling, Rad53 directly phosphorylates Dbf4 and Sld3 to inhibit late-origin firing (Lopez-Mosqueda *et al.* 2010; Zegerman and Diffley 2010). We demonstrated that the *dbf4-NΔ109* mutant defective in the Rad53–Dbf4 interaction coupled with the *sld3-38A* mutant allows late-origin firing in the presence of HU (Figure 7). Since Dbf4-NΔ94 was phosphorylated in HU but the Dbf4-NΔ109 mutant was not (Gabrielse *et al.* 2006) (Figure 7), both pieces of data reveal the importance of residues 95–109 for interaction with Rad53. Together, these data strongly suggest that the Rad53-mediated Dbf4 phosphorylation during the replication checkpoint depends on the physical interaction between Dbf4 and Rad53. Interestingly, mutation of the Rad53 FHA1 domain also impairs late-origin regulation in HU (Pike *et al.* 2004), raising the possibility that Rad53 FHA1 interactions are critical for binding both Dbf4 and Sld3.

Regulation of DDK in the replication checkpoint may involve two phosphorylation events. First, phosphorylation of Dbf4 residue T105 by an unknown kinase could promote the Rad53–DDK interaction. In support of this, T105 was identified as a Rad53 site *in vitro*, and so Rad53 may phosphorylate this site to promote its own binding to Dbf4 (Lopez-Mosqueda *et al.* 2010). Determining whether T105 is phosphorylated *in vivo* and, if so, determining the kinase that phosphorylates T105 is an important future goal. Second, Rad53 then phosphorylates Dbf4 at critical sites downstream of its binding site. Since Rad53 cannot bind to or significantly phosphorylate Dbf4-NΔ109, our data raise the possibility that stable binding of Rad53 to other targets may be needed for efficient phosphorylation. This is similar, for example, to DDK itself, which is targeted to Mcm4 through an N-terminal sequence (Sheu and Stillman 2010).

Acknowledgments

We thank FuJung Chang (Van Andel Research Institute) and Feng-Ling Tsai (University of Pittsburgh) for technical help or advice. We also thank John Diffley and Jörg Heierhorst for yeast strains.

Literature Cited

Ashe, M., R. A. de Bruin, T. Kalashnikova, W. H. McDonald, J. R. Yates, III *et al.*, 2008 The SBF- and MBF-associated protein Msa1 is required for proper timing of G1-specific transcription in Saccharomyces cerevisiae. J. Biol. Chem. 283: 6040–6049.

Bartek, J., C. Lukas, and J. Lukas, 2004 Checking on DNA damage in S phase. Nat. Rev. Mol. Cell Biol. 5: 792–804.

Bastos de Oliveira, F. M., M. R. Harris, P. Brazauskas, R. A. de Bruin, and M. B. Smolka, 2012 Linking DNA replication checkpoint to MBF cell-cycle transcription reveals a distinct class of G1/S genes. EMBO J. 31: 1798–1810.

Boos, D., L. Sanchez-Pulido, M. Rappas, L. H. Pearl, A. W. Oliver *et al.*, 2011 Regulation of DNA replication through Sld3-Dpb11 interaction is conserved from yeast to humans. Curr. Biol. 21: 1152–1157.

Branzei, D., and M. Foiani, 2009 The checkpoint response to replication stress. DNA Repair (Amst.) 8: 1038–1046.

Branzei, D., and M. Foiani, 2010 Maintaining genome stability at the replication fork. Nat. Rev. Mol. Cell Biol. 11: 208–219.

Byeon, I. J., S. Yongkiettrakul, and M. D. Tsai, 2001 Solution structure of the yeast Rad53 FHA2 complexed with a phosphothreonine peptide pTXXL: comparison with the structures of FHA2-pYXL and FHA1-pTXXD complexes. J. Mol. Biol. 314: 577–588.

Caldecott, K. W., 2003 Cell signaling. The BRCT domain: Signaling with friends? Science 302: 579–580.

Chen, Y. C., and M. Weinreich, 2010 Dbf4 regulates the Cdc5 Polo-like kinase through a distinct non-canonical binding interaction. J. Biol. Chem. 285: 41244–41254.

Cheng, L., T. Collyer, and C. F. Hardy, 1999 Cell cycle regulation of DNA replication initiator factor Dbf4p. Mol. Cell. Biol. 19: 4270–4278.

Costanzo, V., D. Shechter, P. J. Lupardus, K. A. Cimprich, M. Gottesman *et al.*, 2003 An ATR- and Cdc7-dependent DNA damage checkpoint that inhibits initiation of DNA replication. Mol. Cell 11: 203–213.

Cuneo, M. J., S. A. Gabel, J. M. Krahn, M. A. Ricker, and R. E. London, 2011 The structural basis for partitioning of the XRCC1/DNA ligase III-alpha BRCT-mediated dimer complexes. Nucleic Acids Res. 39: 7816–7827.

Desany, B. A., A. A. Alcasabas, J. B. Bachant, and S. J. Elledge, 1998 Recovery from DNA replicational stress is the essential function of the S-phase checkpoint pathway. Genes Dev. 12: 2956–2970.

Dohrmann, P. R., and R. A. Sclafani, 2006 Novel role for checkpoint Rad53 protein kinase in the initiation of chromosomal DNA replication in *Saccharomyces cerevisiae*. Genetics 174: 87–99.

Dohrmann, P. R., G. Oshiro, M. Tecklenburg, and R. A. Sclafani, 1999 RAD53 regulates DBF4 independently of checkpoint function in *Saccharomyces cerevisiae*. Genetics 151: 965–977.

Duch, A., G. Palou, Z. O. Jonsson, R. Palou, E. Calvo *et al.*, 2011 A Dbf4 mutant contributes to bypassing the Rad53-mediated block of origins of replication in response to genotoxic stress. J. Biol. Chem. 286: 2486–2491.

Duncker, B. P., K. Shimada, M. Tsai-Pflugfelder, P. Pasero, and S. M. Gasser, 2002 An N-terminal domain of Dbf4p mediates interaction with both origin recognition complex (ORC) and Rad53p and can deregulate late origin firing. Proc. Natl. Acad. Sci. USA 99: 16087–16092.

Durocher, D., J. Henckel, A. R. Fersht, and S. P. Jackson, 1999 The FHA domain is a modular phosphopeptide recognition motif. Mol. Cell 4: 387–394.

Durocher, D., I. A. Taylor, D. Sarbassova, L. F. Haire, S. L. Westcott *et al.*, 2000 The molecular basis of FHA domain:phosphopeptide binding specificity and implications for phospho-dependent signaling mechanisms. Mol. Cell 6: 1169–1182.

Ferreira, M. F., C. Santocanale, L. S. Drury, and J. F. Diffley, 2000 Dbf4p, an essential S phase-promoting factor, is targeted for degradation by the anaphase-promoting complex. Mol. Cell. Biol. 20: 242–248.

Francis, L. I., J. C. Randell, T. J. Takara, L. Uchima, and S. P. Bell, 2009 Incorporation into the prereplicative complex activates the Mcm2–7 helicase for Cdc7-Dbf4 phosphorylation. Genes Dev. 23: 643–654.

Fu, Y. V., and J. C. Walter, 2010 DNA replication: metazoan Sld3 steps forward. Curr. Biol. 20: R515–R517.

Fung, A. D., J. Ou, S. Bueler, and G. W. Brown, 2002 A conserved domain of Schizosaccharomyces pombe dfp1(+) is uniquely required for chromosome stability following alkylation damage during S phase. Mol. Cell. Biol. 22: 4477–4490.

Gabrielse, C., C. T. Miller, K. H. McConnell, A. DeWard, C. A. Fox *et al.*, 2006 A Dbf4p BRCA1 C-terminal-like domain required for the response to replication fork arrest in budding yeast. Genetics 173: 541–555.

Glover, J. N., R. S. Williams, and M. S. Lee, 2004 Interactions between BRCT repeats and phosphoproteins: tangled up in two. Trends Biochem. Sci. 29: 579–585.

Goldstein, A. L., and J. H. McCusker, 1999 Three new dominant drug resistance cassettes for gene disruption in Saccharomyces cerevisiae. Yeast 15: 1541–1553.

Harkins, V., C. Gabrielse, L. Haste, and M. Weinreich, 2009 Budding yeast Dbf4 sequences required for Cdc7 kinase activation and identification of a functional relationship between the Dbf4 and Rev1 BRCT domains. Genetics 183: 1269–1282.

Hartwell, L. H., and T. A. Weinert, 1989 Checkpoints: controls that ensure the order of cell cycle events. Science 246: 629–634.

Huang, M., Z. Zhou, and S. J. Elledge, 1998 The DNA replication and damage checkpoint pathways induce transcription by inhibition of the Crt1 repressor. Cell 94: 595–605.

Kihara, M., W. Nakai, S. Asano, A. Suzuki, K. Kitada *et al.*, 2000 Characterization of the yeast Cdc7p/Dbf4p complex purified from insect cells. Its protein kinase activity is regulated by Rad53p. J. Biol. Chem. 275: 35051–35062.

Labib, K., 2010 How do Cdc7 and cyclin-dependent kinases trigger the initiation of chromosome replication in eukaryotic cells? Genes Dev. 24: 1208–1219.

Labib, K., and G. De Piccoli, 2011 Surviving chromosome replication: the many roles of the S-phase checkpoint pathway. Philos. Trans. R. Soc. Lond. B Biol. Sci. 366: 3554–3561.

Lee, A. Y., T. Chiba, L. N. Truong, A. N. Cheng, J. Do *et al.*, 2012 Dbf4 is direct downstream target of ataxia telangiectasia mutated (ATM) and ataxia telangiectasia and Rad3-related (ATR) protein to regulate intra-S-phase checkpoint. J. Biol. Chem. 287: 2531–2543.

Li, J. M., M. T. Tetzlaff, and S. J. Elledge, 2008 Identification of MSA1, a cell cycle-regulated, dosage suppressor of drc1/sld2 and dpb11 mutants. Cell Cycle 7: 3388–3398.

Liang, X., and S. R. Van Doren, 2008 Mechanistic insights into phosphoprotein-binding FHA domains. Acc. Chem. Res. 41: 991–999.

Liao, H., I. J. Byeon, and M. D. Tsai, 1999 Structure and function of a new phosphopeptide-binding domain containing the FHA2 of Rad53. J. Mol. Biol. 294: 1041–1049.

Longtine, M. S., A. McKenzie, III, D. J. Demarini, N. G. Shah, A. Wach *et al.*, 1998 Additional modules for versatile and economical PCR-based gene deletion and modification in Saccharomyces cerevisiae. Yeast 14: 953–961.

Lopez-Mosqueda, J., N. L. Maas, Z. O. Jonsson, L. G. Defazio-Eli, J. Wohlschlegel *et al.*, 2010 Damage-induced phosphorylation of Sld3 is important to block late origin firing. Nature 467: 479–483.

Mahajan, A., C. Yuan, H. Lee, E. S. Chen, P. Y. Wu *et al.*, 2008 Structure and function of the phosphothreonine-specific FHA domain. Sci. Signal. 1: re12.

Majka, J., A. Niedziela-Majka, and P. M. Burgers, 2006 The checkpoint clamp activates Mec1 kinase during initiation of the DNA damage checkpoint. Mol. Cell 24: 891–901.

Mantiero, D., A. Mackenzie, A. Donaldson, and P. Zegerman, 2011 Limiting replication initiation factors execute the tempo-

ral programme of origin firing in budding yeast. EMBO J. 30: 4805–4814.
Masai, H., N. Sato, T. Takeda, and K. Arai, 1999 CDC7 kinase complex as a molecular switch for DNA replication. Front. Biosci. 4: D834–D840.
Matos, J., J. J. Lipp, A. Bogdanova, S. Guillot, E. Okaz *et al.*, 2008 Dbf4-dependent CDC7 kinase links DNA replication to the segregation of homologous chromosomes in meiosis I. Cell 135: 662–678.
Matthews, L. A., D. R. Jones, A. A. Prasad, B. P. Duncker, and A. Guarne, 2012 Saccharomyces cerevisiae Dbf4 has unique fold necessary for interaction with Rad53 kinase. J. Biol. Chem. 287: 2378–2387.
Miller, C. T., C. Gabrielse, Y. C. Chen, and M. Weinreich, 2009 Cdc7p-Dbf4p regulates mitotic exit by inhibiting Polo kinase. PLoS Genet. 5: e1000498.
Pike, B. L., S. Yongkiettrakul, M. D. Tsai, and J. Heierhorst, 2003 Diverse but overlapping functions of the two forkhead-associated (FHA) domains in Rad53 checkpoint kinase activation. J. Biol. Chem. 278: 30421–30424.
Pike, B. L., N. Tenis, and J. Heierhorst, 2004 Rad53 kinase activation-independent replication checkpoint function of the N-terminal forkhead-associated (FHA1) domain. J. Biol. Chem. 279: 39636–39644.
Randell, J. C., A. Fan, C. Chan, L. I. Francis, R. C. Heller *et al.*, 2010 Mec1 is one of multiple kinases that prime the Mcm2–7 helicase for phosphorylation by Cdc7. Mol. Cell 40: 353–363.
Rodriguez, M. C., and Z. Songyang, 2008 BRCT domains: phosphopeptide binding and signaling modules. Front. Biosci. 13: 5905–5915.
Segurado, M., and J. A. Tercero, 2009 The S-phase checkpoint: targeting the replication fork. Biol. Cell 101: 617–627.
Shellman, Y. G., I. E. Schauer, G. Oshiro, P. Dohrmann, and R. A. Sclafani, 1998 Oligomers of the Cdc7/Dbf4 protein kinase exist in the yeast cell. Mol. Gen. Genet. 259: 429–436.
Sheu, Y. J., and B. Stillman, 2010 The Dbf4-Cdc7 kinase promotes S phase by alleviating an inhibitory activity in Mcm4. Nature 463: 113–117.
Takeda, T., K. Ogino, K. Tatebayashi, H. Ikeda, K. Arai *et al.*, 2001 Regulation of initiation of S phase, replication checkpoint signaling, and maintenance of mitotic chromosome structures during S phase by Hsk1 kinase in the fission yeast. Mol. Biol. Cell 12: 1257–1274.
Travesa, A., D. Kuo, R. A. de Bruin, T. I. Kalashnikova, M. Guaderrama *et al.*, 2012 DNA replication stress differentially regulates G1/S genes via Rad53-dependent inactivation of Nrm1. EMBO J. 31: 1811–1822.
Tsuji, T., S. B. Ficarro, and W. Jiang, 2006 Essential role of phosphorylation of MCM2 by Cdc7/Dbf4 in the initiation of DNA replication in mammalian cells. Mol. Biol. Cell 17: 4459–4472.
Ullman, E. F., H. Kirakossian, S. Singh, Z. P. Wu, B. R. Irvin *et al.*, 1994 Luminescent oxygen channeling immunoassay: measurement of particle binding kinetics by chemiluminescence. Proc. Natl. Acad. Sci. USA 91: 5426–5430.
Wang, P., I. J. Byeon, H. Liao, K. D. Beebe, S. Yongkiettrakul *et al.*, 2000 II. Structure and specificity of the interaction between the FHA2 domain of Rad53 and phosphotyrosyl peptides. J. Mol. Biol. 302: 927–940.
Weinert, T. A., G. L. Kiser, and L. H. Hartwell, 1994 Mitotic checkpoint genes in budding yeast and the dependence of mitosis on DNA replication and repair. Genes Dev. 8: 652–665.
Weinreich, M., and B. Stillman, 1999 Cdc7p-Dbf4p kinase binds to chromatin during S phase and is regulated by both the APC and the RAD53 checkpoint pathway. EMBO J. 18: 5334–5346.
Zegerman, P., and J. F. Diffley, 2010 Checkpoint-dependent inhibition of DNA replication initiation by Sld3 and Dbf4 phosphorylation. Nature 467: 474–478.
Zhao, X., A. Chabes, V. Domkin, L. Thelander, and R. Rothstein, 2001 The ribonucleotide reductase inhibitor Sml1 is a new target of the Mec1/Rad53 kinase cascade during growth and in response to DNA damage. EMBO J. 20: 3544–3553.

Communicating editor: J. A. Nickoloff

GENETICS

Supporting Information
http://www.genetics.org/lookup/suppl/doi:10.1534/genetics.113.149740/-/DC1

DNA Replication Checkpoint Signaling Depends on a Rad53–Dbf4 N-Terminal Interaction in *Saccharomyces cerevisiae*

Ying-Chou Chen, Jessica Kenworthy, Carrie Gabrielse, Christine Hänni, Philip Zegerman, and Michael Weinreich

DOI: 10.1534/genetics.113.149740

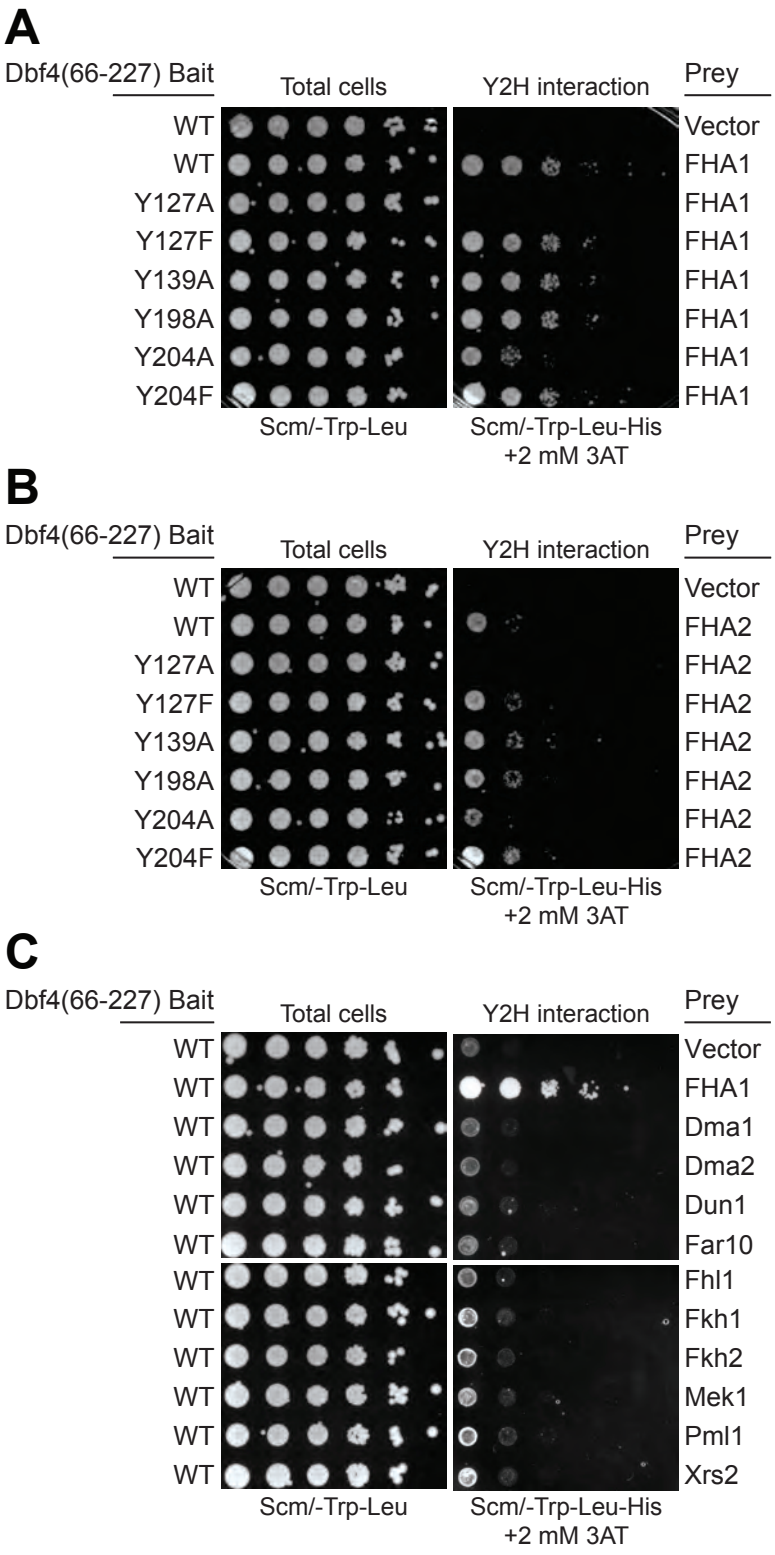
A
Dbf4(66-227) Bait
Total cells
Y2H interaction
Prey
WT
WT
Y127A
Y127F
Y139A
Y198A
Y204A
Y204F
Vector
FHA1
FHA1
FHA1
FHA1
FHA1
FHA1
FHA1
Scm/-Trp-Leu
Scm/-Trp-Leu-His
+2 mM 3AT
B
Dbf4(66-227) Bait
Total cells
Y2H interaction
Prey
WT
WT
Y127A
Y127F
Y139A
Y198A
Y204A
Y204F
Vector
FHA2
FHA2
FHA2
FHA2
FHA2
FHA2
FHA2
Scm/-Trp-Leu
Scm/-Trp-Leu-His
+2 mM 3AT
C
Dbf4(66-227) Bait
Total cells
Y2H interaction
Prey
WT
WT
WT
WT
WT
WT
WT
WT
WT
WT
WT
WT
Vector
FHA1
Dma1
Dma2
Dun1
Far10
Fhl1
Fkh1
Fkh2
Mek1
Pml1
Xrs2
Scm/-Trp-Leu
Scm/-Trp-Leu-His
+2 mM 3AT

Figure S1 Analysis of FHA domain-Dbf4 interactions including a screen of all Y residues in Dbf4 residues 100-227. (A and B) The indicated Dbf4 tyrosine mutants were assayed for a two-hybrid interaction with the Rad53 FHA1 (A) and FHA2 (B) domains. Although Y127A and Y204A mutants eliminate the binding of both FHA domains, there is no loss of binding by substituting the structurally similar but non-phosphorylatable amino acid, phenylalanine (Y127F and Y204F). (C) Two hybrid interaction data of the Dbf4 N-terminus (66-227) with all remaining FHA domains in the yeast genome. Dma1 (pJK135, 137-302aa) (DUROCHER and JACKSON 2002), Dma2 (pJK137, 246-408aa) (DUROCHER and JACKSON 2002), Dun1 (pJK275, 1-160aa) (HAMMET *et al.* 2000), Far10 (pJK277, 61-227aa) (DUROCHER and JACKSON 2002), Fhl1 (pJK279, 253-400aa) (WADE *et al.* 2004), Fkh1 (pJK281, 41-185aa) (DUROCHER and JACKSON 2002), Fkh2 (pJK287, 1-254aa) (DARIEVA *et al.* 2003), Mek1 (pJK283, 1-152aa) (DUROCHER and JACKSON 2002), Pml1 (pJK289, 54-204) (BROOKS *et al.* 2009), Xrs2 (pJK285, 1-125aa) (PALMBOS *et al.* 2008).

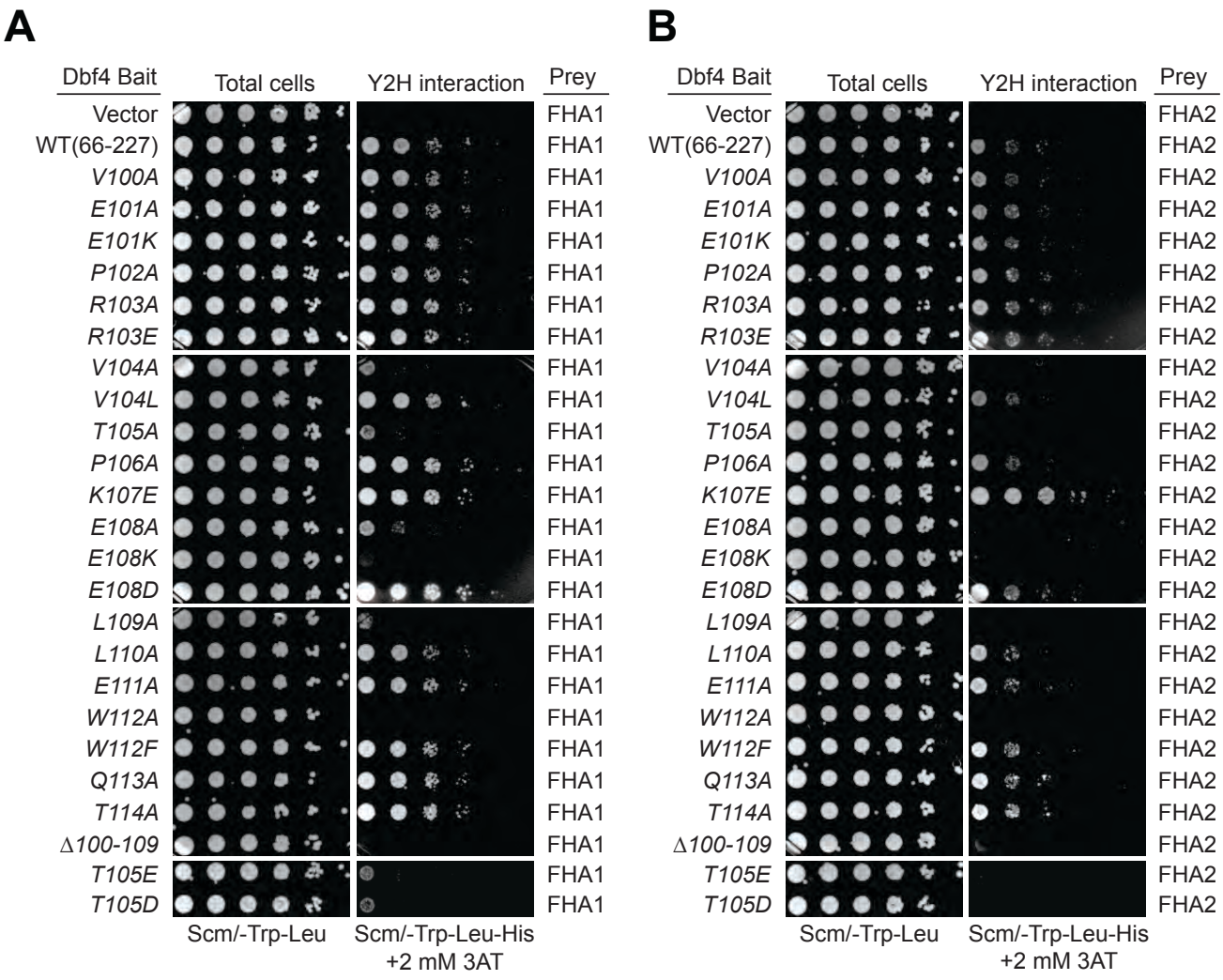

Figure S2 Dbf4 residues V104, T105, E108, L109, and W112 were required for binding the Rad53 FHA domains. The indicated substitutions within residues 100-114 of the Dbf4 Nterminal (66-227) bait plasmid were assayed for a two-hybrid interaction with the Rad53 FHA1 (panel A) and FHA2 domains (panel B). Spotting as in Figure S1.

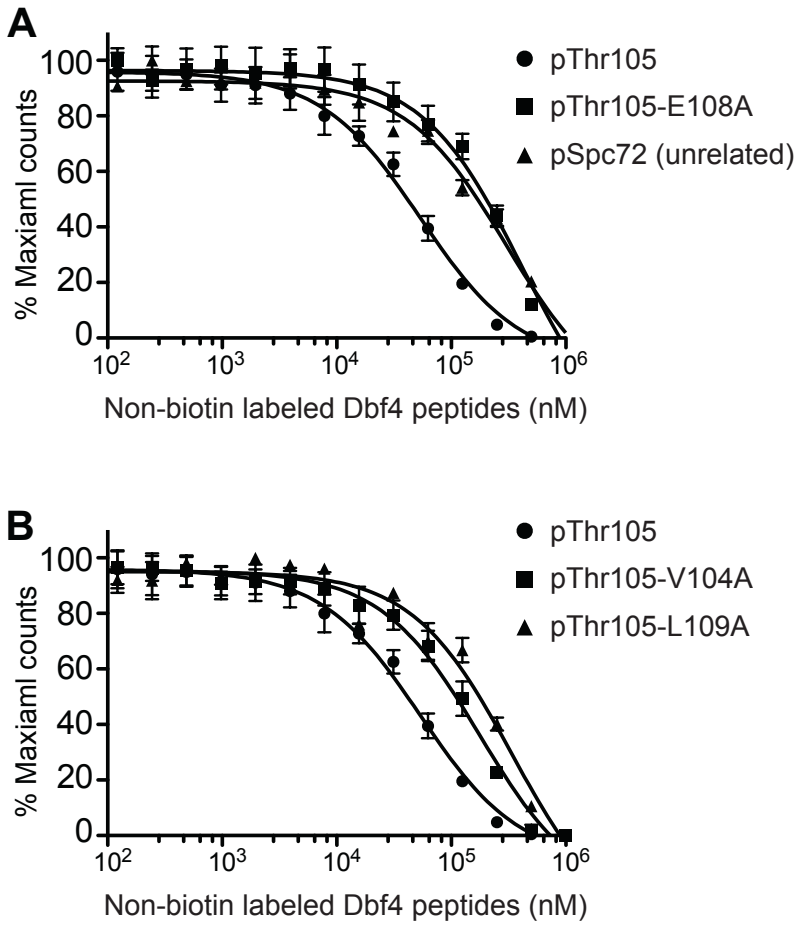

Figure S3 Dbf4 residues V104, E108, and L109 were critical for binding the Rad53 FHA domains. (A) The Dbf4 biotinylated peptide pThr105-FHA1 interaction was competed by the non-biotinylated T105-phosphorylated Dbf4 peptides (pThr105), but not by the same Dbf4 peptide with an E108A substitution, or by an unrelated phospho-serine peptide (pSpc72). (B) The pThr105-V104A and pThr105-L109A peptides were also defective in competing the biotinylated pThr105-FHA1 interaction.

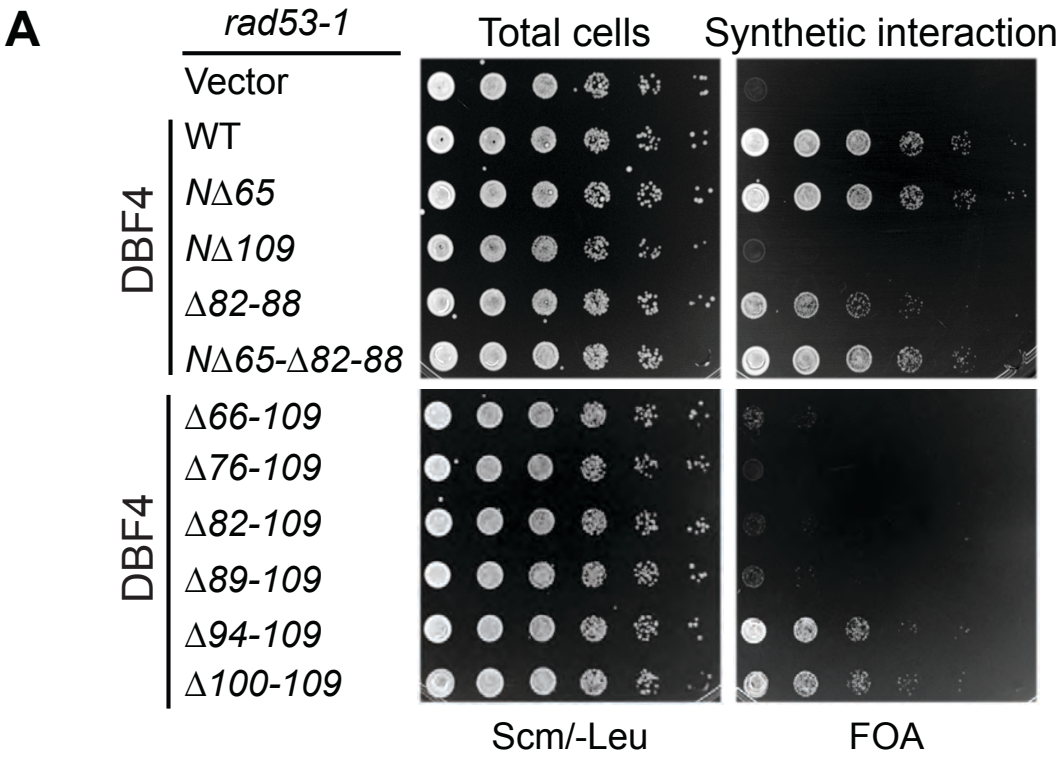
A
rad53-1
Total cells
Synthetic interaction
Vector
DBF4
WT
NΔ65
NΔ109
Δ82-88
NΔ65-Δ82-88
DBF4
Δ66-109
Δ76-109
Δ82-109
Δ89-109
Δ94-109
Δ100-109
Scm/-Leu
FOA

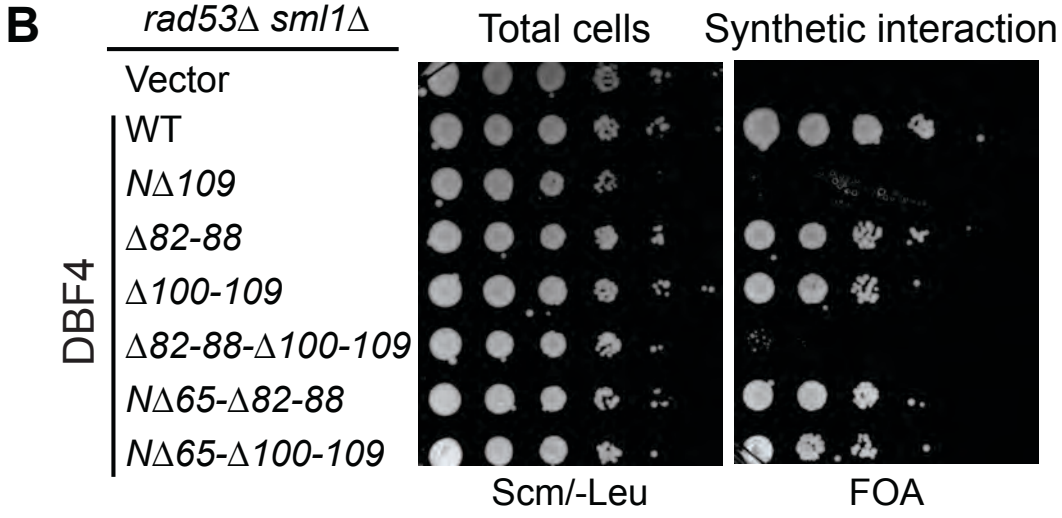
B
rad53Δ sml1Δ
Total cells
Synthetic interaction
Vector
DBF4
WT
NΔ109
Δ82-88
Δ100-109
Δ82-88-Δ100-109
NΔ65-Δ82-88
NΔ65-Δ100-109
Scm/-Leu
FOA

Figure S4 The synthetic lethality between *dbf4-NΔ109* and *rad53-1* or *rad53Δ* was not due to either loss of Cdc5 interaction or increased Dbf4 stability, but requires sequences between residues 82-109. Wild type and various *dbf4* mutants were cloned in low-copy number (*ARS/CEN/LEU2*) vectors, driven by the *DBF4* endogenous promoter. Plasmids were transformed into M1589 (*rad53-1 dbf4Δ::kanMX6 [pDBF4-URA3]*) or M3581 (*rad53Δ::TRP1 sml1Δ::HIS3 dbf4Δ::kanMX6 [pDBF4-URA3]*) and the wild-type *DBF4-URA3* plasmids were selected against on FOA. Cells that could not grow on FOA plates were scored as having a synthetic lethal interaction. The NΔ65 deletion causes increased Dbf4 stability by deleting sequences important for ubiquitin-mediated proteolysis. The Δ82-88 deletion prevented the Cdc5 interaction with Dbf4, while the Δ100-109 deletion prevented the interaction with Rad53 (see Figure S6).

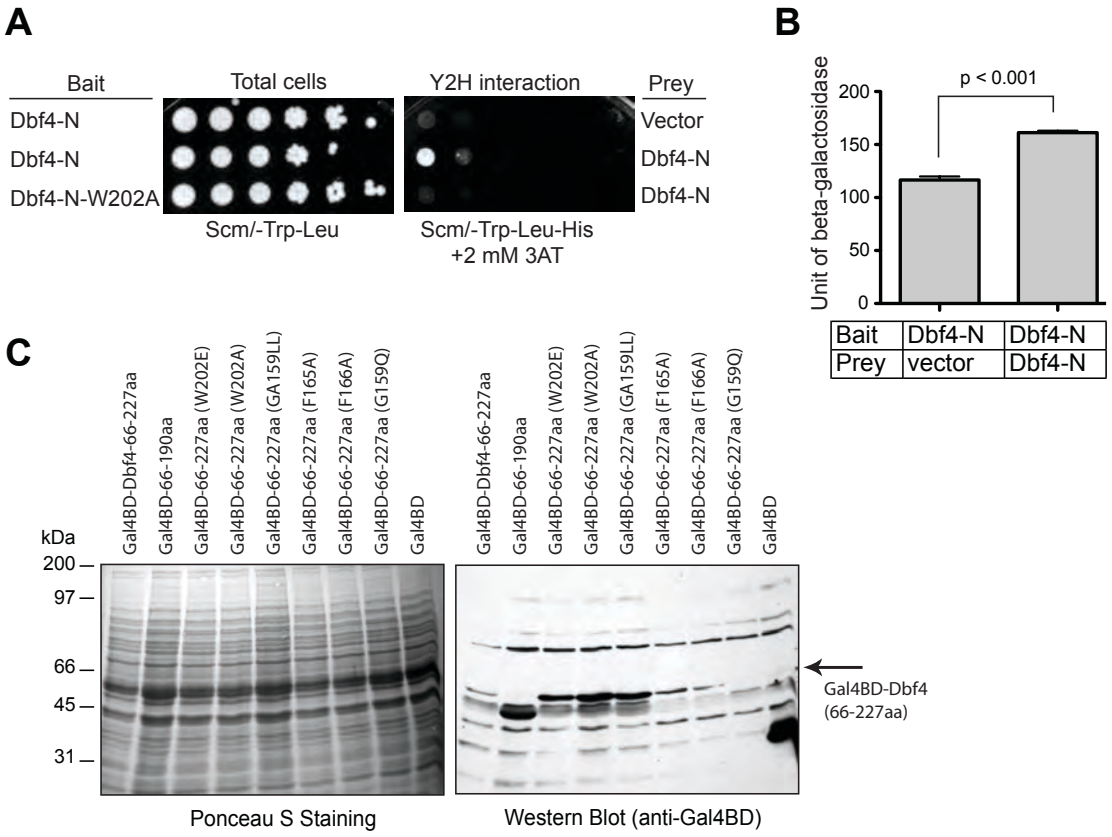

Figure S5 Evidence for a Dbf4-Dbf4 N-terminal interaction. (A-B) Dbf4 N-terminal residues 66-227 were cloned in two-hybrid bait and prey plasmids separately to examine Dbf4 dimerization. Two-hybrid interactions were quantitated by spotting assays on selective media (panel A) or by β-galactosidase assays (panel B). (C) The expression of representative Dbf4 mutants in two-hybrid assays is shown by Western blotting against the c-Myc epitope tag on the Gal4BD (DNA Binding Domain) fusions. Whole cell extracts prepared by TCA extraction method were equally loaded onto each lane (Ponceau S staining, left). Gal4BD fused Dbf4 were detected by anti-Myc antibody (9E10), followed by anti-mouse second antibody (right).

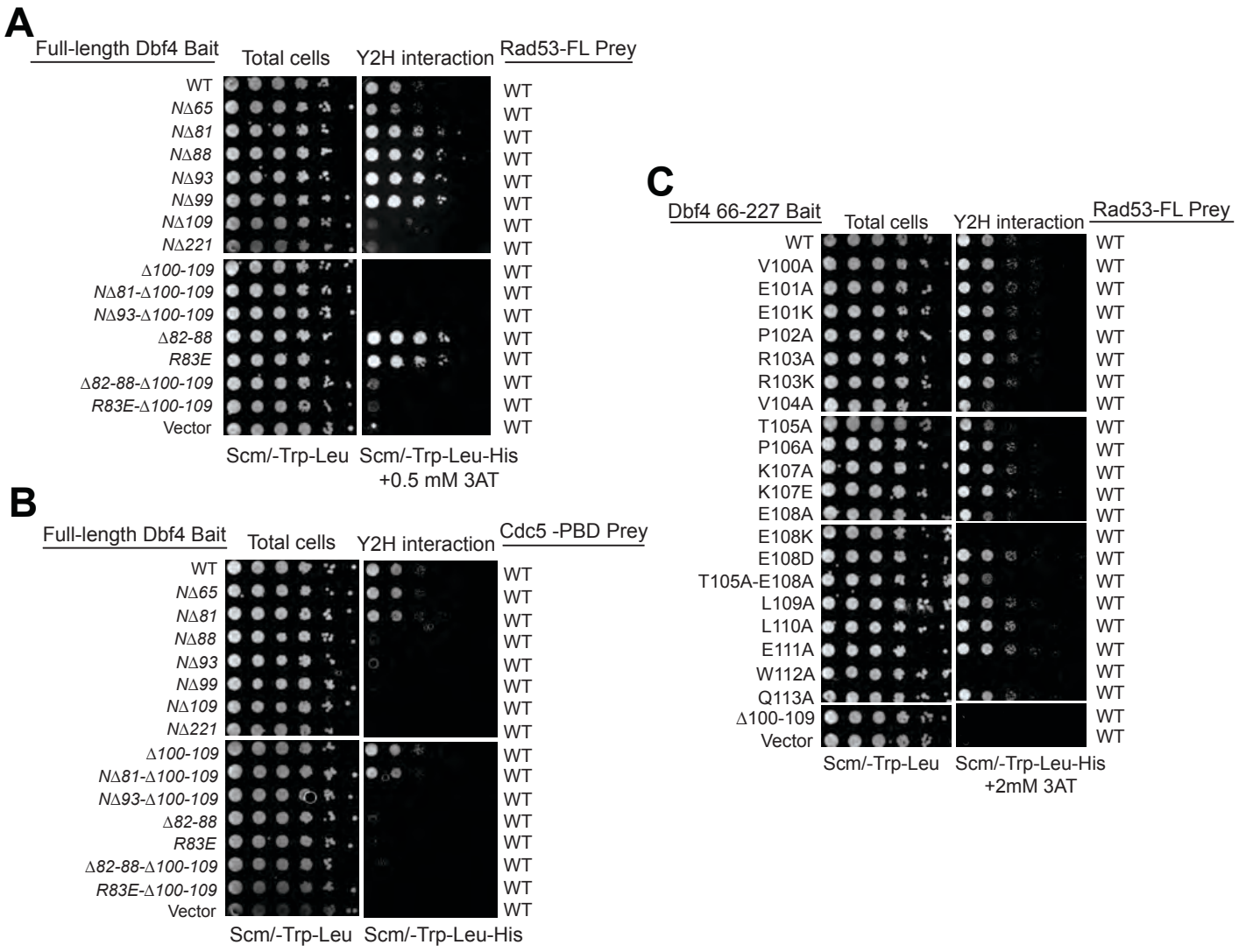

Figure S6 Dbf4 sequences important for binding full length Rad53 and the Cdc5 PBD. (A) A series of deletion in full-length Dbf4 was assayed by two-hybrid for interaction with full length Rad53 (panel A) or with the Cdc5 Polo-box domain (PBD) (panel B). The *dbf4-Δ100-109* deletion caused a loss of Rad53 binding, but still allowed interaction with the Cdc5-PBD. The *dbf4-Δ82-88* deletion caused loss of Cdc5 binding but not Rad53. An N-terminal deletion through residue 81 (NΔ81) or disruption of the Cdc5 binding site (Δ82-88 and R83E) caused increased Rad53 binding compared to full length Dbf4. (C) Dbf4 point mutations were assayed for their two-hybrid interaction against full length Rad53. The Δ100-109 deletion caused a loss of the two-hybrid signal similar to the vector control. The V104A, T105A, E108A mutations resulted in a diminished Rad53 interaction.

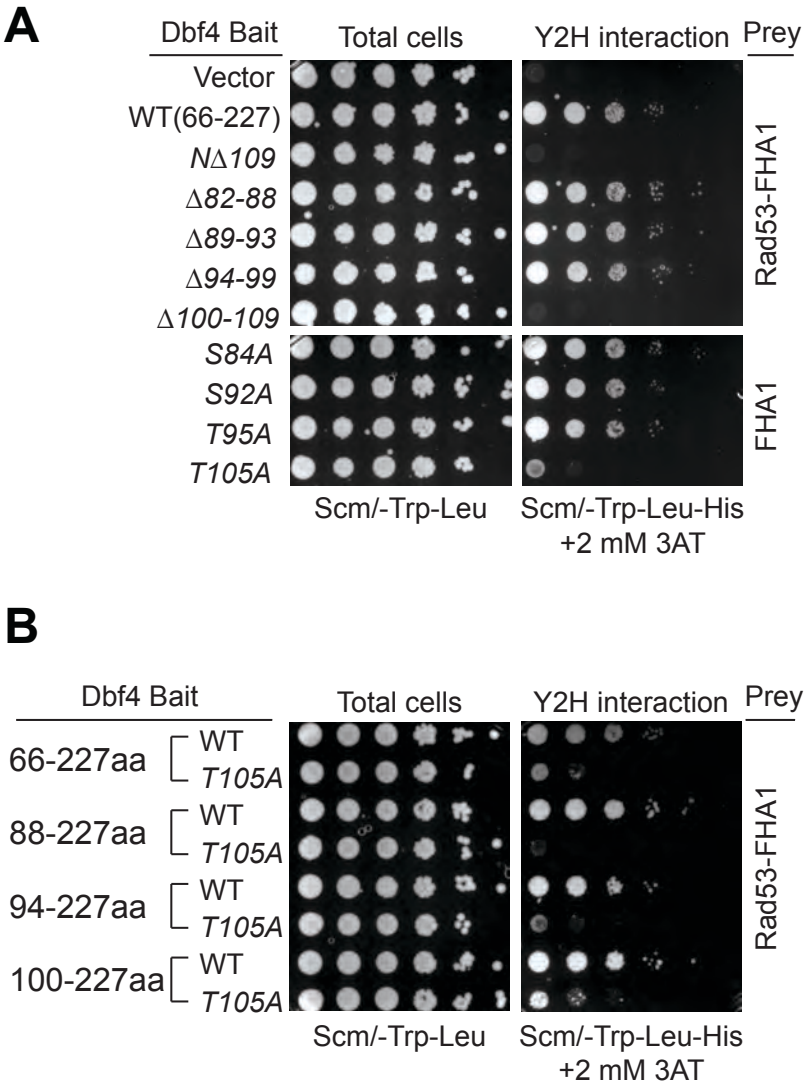

Figure S7 Dbf4 T105 residue was critical for the Dbf4-FHA1 domain interaction. (A) The *dbf4-Δ100-109*, *dbf4-T105A* and *dbf4-NΔ109* mutants caused a loss of FHA1 domain binding in two-hybrid assays. The *dbf4-S84A, -S92A*, and *-T95A* mutants did not show any effect on FHA1 domain binding. (B) Substitution of T105A within various Dbf4 truncations consistently caused a loss of interaction with the FHA1 domain.

Table S1 Plasmids used in this study

Plasmid	Description	Source
p4339	pCRII-TOPO::natRMX4	Goldstein and McCusker, 1999
pAcSG2		BD Biosciences
pCG10	pRS415-*DBF4* $_{N\Delta 109}$	Gabrielse et al., 2006
pCG40	pAcSG2-*DBF4* $_{N\Delta 109}$	Miller et al., 2009
pCG44	pAcSG2-*DBF4* $_{N\Delta 221}$	Gabrielse et al., 2006
pCG52	pGBKT7-*DBF4* $_{66-227}$	Miller et al., 2009
pCG53	pYJ204-*DBF4* $_{N\Delta 65}$	Miller et al., 2009
pCG60	pCG52$_{ADH1\ promoter-\Delta(-732)-(-802)}$	Miller et al., 2009
pCG63	pCG60 W202E	This study
pCG64	pCG60 W202A	This study
pCG74	pYJ204-*DBF4* $_{N\Delta 109}$	Miller et al., 2009
pCG75	pYJ204-*DBF4* $_{N\Delta 221}$	Miller et al., 2009
pCG91	pAcSG2-*DBF4* $_{N\Delta 65}$	Gabrielse et al., 2006
pCG101	pCG60 GA159,160LL	This study
pCG108	pCG60 F165A	This study
pCG110	pCG60 F166A	This study
pCG146	pCG60 G159Q	This study
pCG265	pGAD-C1-*CDC7* $_{1-507}$	Harkins et al., 2009
pCM16	pAcSG2-3myc-*CDC5* $_{65-705}$	Miller et al., 2009
pCM21	pCG60-*DBF4* $_{66-109}$	Miller et al., 2009
pET24a-GST		Chen and Weinreich, 2010
pGAD-C1		James et al. 1996
pGAD-Cdc5.3	pGAD-C1-*CDC5* $_{421-705}$	Miller et al., 2009
pGAD-YOR.3	pGAD-C3-*MSA169-530*	This study
pGBKT7		Clontech
pJK18	pCG60 T171E	This study
pJK20	pCG60 E108A	This study
pJK22	pCG60 T171S	This study
pJK25	pCG60 V100A	This study
pJK26	pCG60 R103A	This study
pJK27	pCG60 V104A	This study
pJK29	pCG60 P106A	This study
pJK31	pCG60 L109A	This study
pJK33	pCG60 K107A	This study
pJK34	pCG60 T105A E108A	This study
pJK36	pCG60 E108K	This study
pJK37	pCG60 T171A	This study
pJK39	pCG60 E101A	This study
pJK41	pCG60 P102A	This study

pJK45	pYJ204-*DBF4* $_{NΔ81}$	This study
pJK47	pYJ204-*DBF4* $_{NΔ93}$	This study
pJK48	pYJ204-*DBF4* $_{NΔ99}$	This study
pJK49	pCG60 T105S	This study
pJK51	pCG60 K107E	This study
pJK53	pCG60 T131A	This study
pJK55	pCG60 L110A	This study
pJK57	pCG60 E111A	This study
pJK59	pCG60 W112A	This study
pJK61	pCG60 T114A	This study
pJK67	pCG60-*DBF4* $_{Δ94-99}$	This study
pJK76	pYJ204-*DBF4* $_{NΔ88}$	This study
pJK82	pCG60 V104L	This study
pJK83	pCG60 L109V	This study
pJK85	pCG60 W112F	This study
pJK86	pCG60 T188A	This study
pJK89	pCG60 T157A	This study
pJK91	pCG60 T163A	This study
pJK93	pCG60 TT168,169AA	This study
pJK95	pCG60 T175A	This study
pJK97	pYJ319 G653E	This study
pJK99	pYJ319 T654A	This study
pJK101	pYJ319 N655A	This study
pJK103	pYJ380 G653E	This study
pJK105	pYJ380 T654A	This study
pJK107	pYJ380 N655A	This study
pJK108	pCG60 Y127A	This study
pJK110	pCG60 Y139A	This study
pJK112	pCG60 Y198A	This study
pJK114	pCG60 Y204A	This study
pJK121	pCG60 Y127S	This study
pJK122	pCG60 Y127T	This study
pJK124	pCG60 I130A	This study
pJK125	pCG60 T171V	This study
pJK126	pCG60 Y204F	This study
pJK128	pCG60 Y127F	This study
pJK135	pGAD-C1-*DMA1* $_{137-302}$	This study
pJK137	pGAD-C1-*DMA2* $_{246-408}$	This study
pJK149	pCG60 T95A	Chen and Weinreich, 2010
pJK169	pET24a-GST-*RAD53* $_{2-164}$	This study
pJK170	pET24a-GST-*RAD53* $_{2-175}$	This study
pJK171	pET24a-GST-*RAD53* $_{2-279}$	This study

pJK179	pCG60-*DBF4* $_{N\Delta87}$ T105A	This study
pJK181	pCG60-*DBF4* $_{N\Delta99}$ T105A	This study
pJK185	pCG60-*DBF4* $_{N\Delta93}$ T105A	This study
pJK269	pET24a-GST-*RAD53* $_{2-164}$ R70A	This study
pJK275	pGAD-C1-*DUN1* $_{1-160}$	This study
pJK277	pGAD-C1-*FAR10* $_{61-227}$	This study
pJK279	pGAD-C1-*FHL1* $_{253-400}$	This study
pJK281	pGAD-C1-*FKH1* $_{41-185}$	This study
pJK283	pGAD-C1-*MEK1* $_{1-152}$	This study
pJK285	pGAD-C1-*XRS2* $_{1-125}$	This study
pJK287	pGAD-C1-*FKH2* $_{1-254}$	This study
pJK289	pGAD-C1-*PML1* $_{54-204}$	This study
pJK380	pET24a-GST-*RAD53* $_{483-821}$	This study
pJK382	pET24a-GST-*RAD53* $_{549-730}$	This study
pJK410	pYJ380 R605A	This study
pJK420	pET24a-GST-*RAD53* $_{523-821}$	This study
pJK468	pCG60 R209E	This study
pJK469	pCG60 K212E	This study
pJK487	pCG60 K206E	This study
pJK542	pRS415-DBF4$_{N\Delta94}$	This study
pJK544	pCG60-DBF4$_{N\Delta94}$	This study
pMW1	pAcPK30-*DBF4* $_{1-704}$	Gabrielse et al., 2006
pMW47	pAcSG2-HAHIS6-*CDC7* $_{1-507}$	Gabrielse et al., 2006
pMW489	pRS415-*DBF4* $_{1-704}$	Gabrielse et al., 2006
pMW490	pRS416-*DBF4* $_{1-704}$	Gabrielse et al., 2006
pMW526	pRS415-*DBF4* $_{N\Delta65}$	Gabrielse et al., 2006
pRS415	*LEU2 ARS-CEN*	Sikorski and Hieter, 1989
pRS416	*URA3 ARS-CEN*	Sikorski and Hieter, 1989
pYJ3	pCG60-*DBF4* $_{\Delta67-81}$	Chen and Weinreich, 2010
pYJ4	pCG60-*DBF4* $_{\Delta67-88}$	Chen and Weinreich, 2010
pYJ5	pCG60-*DBF4* $_{\Delta67-93}$	Chen and Weinreich, 2010
pYJ6	pCG60-*DBF4* $_{\Delta67-99}$	Chen and Weinreich, 2010
pYJ7	pCG60-*DBF4* $_{\Delta67-103}$	Chen and Weinreich, 2010
pYJ8	pCG60-*DBF4* $_{\Delta67-107}$	Chen and Weinreich, 2010
pYJ9	pCG60-*DBF4* $_{N\Delta109}$	Chen and Weinreich, 2010
pYJ16	pCG60 S84A	Chen and Weinreich, 2010
pYJ30	pCG60 R83E	Chen and Weinreich, 2010
pYJ38	pCG60-*DBF4* $_{\Delta82-88}$	Miller et al., 2009
pYJ74	pMW489-*DBF4* $_{\Delta82-88}$	Chen and Weinreich, 2010
pYJ167	pCG60 S92A	Chen and Weinreich, 2010
pYJ182	pAcSG2-*DBF4* $_{\Delta82-88}$	Chen and Weinreich, 2010
pYJ193	pMW489-*DBF4* $_{\Delta76-109}$	This study

pYJ195	pMW489-*DBF4* $_{\Delta 82\text{-}109}$	This study
pYJ198	pMW489-*DBF4* $_{\Delta 66\text{-}109}$	This study
pYJ201	pMW489-*DBF4* $_{N\Delta 65\text{-}\Delta 82\text{-}88}$	Chen and Weinreich, 2010
pYJ204	pGBKT7-*DBF4* $_{1\text{-}704}$	Miller et al., 2009
pYJ206	pYJ204-*DBF4* $_{\Delta 82\text{-}88}$	Miller et al., 2009
pYJ218	pMW489-*DBF4* $_{\Delta 89\text{-}109}$	This study
pYJ219	pMW489-*DBF4* $_{\Delta 100\text{-}109}$	This study
pYJ222	pMW489-*DBF4* $_{\Delta 94\text{-}109}$	This study
pYJ308	pGAD-C1-*RAD53* $_{1\text{-}300}$	This study
pYJ319	pGAD-C1-*RAD53* $_{1\text{-}821}$	This study
pYJ326	pCG60-*DBF4* $_{\Delta 89\text{-}93}$	Chen and Weinreich, 2010
pYJ332	pCG60-*DBF4* $_{\Delta 100\text{-}109}$	This study
pYJ336	pCG60 T105A	This study
pYJ340	pMW489-*DBF4* $_{\Delta 82\text{-}88\text{-}\Delta 100\text{-}109}$	This study
pYJ355	pYJ308 R70A	This study
pYJ368	pCG60-*DBF4* $_{66\text{-}190}$	This study
pYJ372	pCG60-*DBF4* $_{66\text{-}150}$	This study
pYJ380	pGAD-C1-*RAD53* $_{483\text{-}821}$	This study
pYJ384	pYJ319 R70A	This study
pYJ388	pYJ319 R605A	This study
pYJ392	pCG60 T105E	This study
pYJ394	pCG60 T105D	This study
pYJ422	pAcSG2-*DBF4* $_{\Delta 100\text{-}109}$	This study
pYJ424	pAcSG2-*DBF4* $_{\Delta 82\text{-}88\text{-}\Delta 100\text{-}109}$	This study
pYJ426	pMW489-*DBF4* $_{N\Delta 65\text{-}\Delta 100\text{-}109}$	This study
pYJ428	pAcSG2-*RAD53* $_{1\text{-}821}$	This study
pYJ461	pYJ204 R83E	This study
pYJ462	pYJ204-*DBF4* $_{\Delta 100\text{-}109}$ R83E	This study
pYJ464	pYJ204-*DBF4* $_{\Delta 100\text{-}109}$	This study
pYJ466	pYJ204-*DBF4* $_{\Delta 82\text{-}88\text{-}\Delta 100\text{-}109}$	This study
pYJ489	pCG60 E101K	This study
pYJ491	pCG60 R103E	This study
pYJ493	pCG60 Q113A	This study
pYJ494	pYJ204-*DBF4* $_{N\Delta 81\text{-}\Delta 100\text{-}109}$	This study
pYJ497	pYJ204-*DBF4* $_{N\Delta 93\text{-}\Delta 100\text{-}109}$	This study
pYJ507	pCG60 E108D	This study
pYJ512	pCG60 T138A	This study
pYJ535	pGAD-C1-*DBF4* $_{66\text{-}227}$	This study

Table S2 Yeast strains used in this study

Stain	Genotype	Source
PJ69-4A	*MAT* **a** *trp1-901 leu2-3, -112 ura3-52 his3-200 gal4Δ gal80Δ LYS2::GAL1-HIS3 GAL2-ADE2 met2::GAL7-lacZ*	James et al., 1996
W303-1A	*MAT* **a** *ade2-1, ura3-1 his3-11, -15 trp1-1 leu2-3, -112 can1-100 rad5-535*	Thomas and Rothstein, 1989
y57	W303 *MAT* **a** *rad53-R70A sml1Δ::HIS3 RAD5*	Pike et al., 2004
y59	W303 *MAT* **a** *rad53-K227A sml1Δ::HIS3 RAD5*	Pike et al., 2004
y205	W303 *MAT* **a** *rad53-R605A sml1Δ::HIS3 RAD5*	Pike et al., 2004
y1853	W303 *MAT* **a** *sml1Δ::URA3 sld3-38A-10his-13MYC::kanMX4*	Zegerman and Diffley, 2010
y2573	W303 *MAT* **a** *dbf4Δ::TRP1 his3::PDBF4-dbf4 4A::HIS3 sld3-38A-10his-13MYC::kanMX4*	Zegerman and Diffley, 2010
M517	W303 *MAT* **a** *rad53-1*	Gabrielse at al., 2006
M895	W303 *MAT* **a** *dbf4Δ::kanMX6* [pMW490; pRS416-*DBF4 URA3*]	Gabrielse at al., 2006
M927	W303 *MAT* **a** *dbf4Δ::kanMX4 3HA-CDC7-TRP1* [pMW490; pRS416-*DBF4-URA3*]	Gabrielse at al., 2006
M932	W303 *MAT* **a** *dbf4Δ::kanMX4 3HA-CDC7-TRP1* [pMW489; pRS415-*DBF4-LEU2*]	Gabrielse at al., 2006
M936	W303 *MAT* **a** *dbf4Δ::kanMX4 3HA-CDC7-TRP1* [pCG10; pRS415-DBF4-*NΔ109-LEU2*]	Gabrielse at al., 2006
M2864	W303 *MAT* **a** *dbf4Δ::kanMX4 3HA-CDC7-TRP1* [pCG10; pRS415-DBF4-*NΔ94-LEU2*]	This study
M1261	W303 *MAT* **a** *dbf4-NΔ109*	Gabrielse at al., 2006
M1589	W303 *MAT* **a** *rad53-1 dbf4Δ::kanMX6* [pMW490; pRS416-*DBF4 URA3*]	Gabrielse at al., 2006
M1800	W303 *MAT1 dbf4-NΔ109-kanMX6*	Miller et al., 2009
M3581	W303 *MAT* **a** *rad53Δ::TRP1 sml1Δ::HIS3 dbf4Δ::kanMX6* [pMW490; pRS416-*DBF4 URA3*]	This study
M3831	W303 *MAT* **a** *RAD53-3MYC-TRP1*	This study
M3890	W303 *MAT* **a** *dbf4-NΔ109-natMX4*	This study
M3905	W303 *MAT* **a** *dbf4-NΔ109-natMX4 sld3-38A-10his-13MYC::kanMX4*	This study
M3913	W303 *MAT* **a** *dbf4-NΔ109-kanMX6 sml1::HIS3*	This study
M3920	W303 *MAT* **α** *RAD53-3MYC-TRP1 dbf4-NΔ109-kanMX6 sml1Δ::HIS3*	This study

Table S3 Peptides used in this study

Peptide name	Peptide sequence	Length	MW
Biotin-Dbf4 (98-113)	Biotin- KNV EPR VTP KEL LEW Q	Biotin + 17	2192.9
Biotin-pDbf4	Biotin- KNV EPR V(pT)P KEL LEW Q	Biotin + 17	2273.2
Dbf4 (98-113)	KNV EPR VTP KEL LEW Q	17	1966.4
pDbf4 (pThr105)	KNV EPR V(pT)P KEL LEW Q	17	2047.5
pDbf4-V104A	KNV EPR A(pT)P KEL LEW Q	17	2019.8
pDbf4-E108A	KNV EPR V(pT)P KAL LEW Q	17	1989.9
pDbf4-E108D	KNV EPR V(pT)P KDL LEW Q	17	2032.7
pDbf4-L109A	KNV EPR V(pT)P KEA LEW Q	17	2005
Biotin-Rad9	IMS EVE LTQ ELP EVE	15	1972.28
Biotin-pRad9	IMS EVE L(pT)Q ELP EVE	15	2052.26
pSpc72	EEF LSL AQS (pS)PA GSQ LES RD	20	2231.3

Supplemental references

BROOKS, M. A., A. DZIEMBOWSKI, S. QUEVILLON-CHERUEL, V. HENRIOT, C. FAUX *et al.*, 2009 Structure of the yeast Pml1 splicing factor and its integration into the RES complex. Nucleic Acids Res **37:** 129-143.

CHEN, Y. C., and M. WEINREICH, 2010 Dbf4 regulates the Cdc5 Polo-like kinase through a distinct non-canonical binding interaction. J Biol Chem **285:** 41244-41254.

DARIEVA, Z., A. PIC-TAYLOR, J. BOROS, A. SPANOS, M. GEYMONAT *et al.*, 2003 Cell cycle-regulated transcription through the FHA domain of Fkh2p and the coactivator Ndd1p. Curr Biol **13:** 1740-1745.

DUROCHER, D., and S. P. JACKSON, 2002 The FHA domain. FEBS Lett **513:** 58-66.

GABRIELSE, C., C. T. MILLER, K. H. MCCONNELL, A. DEWARD, C. A. FOX *et al.*, 2006 A Dbf4p BRCA1 C-terminal-like domain required for the response to replication fork arrest in budding yeast. Genetics **173:** 541-555.

GOLDSTEIN, A. L., and J. H. MCCUSKER, 1999 Three new dominant drug resistance cassettes for gene disruption in Saccharomyces cerevisiae. Yeast **15:** 1541-1553.

HAMMET, A., B. L. PIKE, K. I. MITCHELHILL, T. TEH, B. KOBE *et al.*, 2000 FHA domain boundaries of the dun1p and rad53p cell cycle checkpoint kinases. FEBS Lett **471:** 141-146.

HARKINS, V., C. GABRIELSE, L. HASTE and M. WEINREICH, 2009 Budding yeast Dbf4 sequences required for Cdc7 kinase activation and identification of a functional relationship between the Dbf4 and Rev1 BRCT domains. Genetics **183:** 1269-1282.

JAMES, P., J. HALLADAY and E. A. CRAIG, 1996 Genomic libraries and a host strain designed for highly efficient two-hybrid selection in yeast. Genetics **144:** 1425-1436.

MILLER, C. T., C. GABRIELSE, Y. C. CHEN and M. WEINREICH, 2009 Cdc7p-Dbf4p regulates mitotic exit by inhibiting Polo kinase. PLoS Genet **5:** e1000498.

PALMBOS, P. L., D. WU, J. M. DALEY and T. E. WILSON, 2008 Recruitment of Saccharomyces cerevisiae Dnl4-Lif1 complex to a double-strand break requires interactions with Yku80 and the Xrs2 FHA domain. Genetics **180:** 1809-1819.

PIKE, B. L., S. YONGKIETTRAKUL, M. D. TSAI and J. HEIERHORST, 2004 Mdt1, a novel Rad53 FHA1 domain-interacting protein, modulates DNA damage tolerance and G(2)/M cell cycle progression in Saccharomyces cerevisiae. Mol Cell Biol **24:** 2779-2788.

THOMAS, B. J., and R. ROTHSTEIN, 1989 Elevated recombination rates in transcriptionally active DNA. Cell **56:** 619-630.

WADE, J. T., D. B. HALL and K. STRUHL, 2004 The transcription factor Ifh1 is a key regulator of yeast ribosomal protein genes. Nature **432:** 1054-1058.

ZEGERMAN, P., and J. F. DIFFLEY, 2010 Checkpoint-dependent inhibition of DNA replication initiation by Sld3 and Dbf4 phosphorylation. Nature **467:** 474-478.